# MANIPULATING ANTIBODY-ANTIGEN INTERACTIONS IN MICROPOROUS MEMBRANES FOR SELECTIVE ANTIBODY AND PROTEIN PURIFICATION

By

Austin Landry Bennett

A THESIS

Submitted to
Michigan State University
in partial fulfillment of the requirements
for the degree of

Chemistry – Master of Science

2016

## ABSTRACT

MANIPULATING ANTIBODY-ANTIGEN INTERACTIONS IN MICROPOROUS MEMBRANES FOR SELECTIVE ANTIBODY AND PROTEIN PURIFICATION

By

Austin Landry Bennett

Monoclonal antibodies are among the most successful and most expensive therapeutic agents. Rapid, inexpensive antibody capture should decrease the cost of both production and detection of these remarkable drugs. Affinity membranes can potentially capture protein more rapidly than traditional bead-based methods without the large pressure drops of columns.

This research employed an Fc (fragment, crystallizable) binding peptide (denoted as KK12) and an Fab (fragment, antigen-binding) binding peptide (denoted as K19) for rapid antibody capture in membranes. KK12-modified membranes captured 8.40 mg of Herceptin and 9.96 mg of Avastin per mL of membrane. The antibodies eluted in 100 mM Gly (pH 2.7), but the membranes were not reusable. K19-modified membranes capture 16.3 mg of Herceptin per mL of membrane and showed minimal binding of Avastin. Furthermore, K19-modified membranes selectively captured Herceptin from human serum and showed no significant non-specific adsorption.

Antibody-containing membranes may also enable rapid, high-throughput immunoprecipitation. Anti-(hemagglutinin A) (HA) antibodies successfully captured HA-tagged regulator G-protein signaling 2 (HA-RGS2) from cell lysate and HA-RGS2 subsequently eluted in 5% formic acid. Non-specific adsorption, however, is a persistent problem that must be addressed. Anti-(C-peptide) antibodies captured up to 4 pmoles of C-peptide. This is a promising result for future studies that aim to determine the role of C-peptide in diabetic complications.

## ACKNOWLEDGEMENTS

I would like to first and foremost thank Dr. Merlin Bruening for his guidance and oversight throughout my time at Michigan State University. Dr. Bruening is a gifted scientist but perhaps an even better mentor. He liberally graced me with "tutelage from his hand," teaching me not just how to perform protocols in the lab but also how to think critically and logically about the work I was doing. Lastly, I thank Dr. Bruening for his unwavering support over the past two years, specifically with respect to my decision to leave with my M.S. degree. I cannot thank him enough for being a mentor, advisor and role model for me during my time in his research lab.

I must also acknowledge my Bruening research group members for their character and commitment to their work. My lab mates created an environment of excellence that has resulted in some exciting research. I would like to specifically thank Wenjing Ning for mentoring me during my first year as a graduate student and teaching me everything I know about membrane science and bioanalytical separations. Much of the work contained herein was conducted with the assistance and at the direction of Wenjing. I appreciate her patience with me over the past two years as I slowly learned to be a proper scientist. I would also like to specifically thank Dr. Yaghoub Mansourpanah of Lorestan University for his help while visiting the Bruening Lab in 2016.

I must give special thanks to Dr. Dana Spence and Cody Pinger for both their friendship and their assistance with the C-peptide capture project.

Lastly, I must recognize my beautiful girlfriend Larissa and my amazing family. Without their love and support, I would have never made it to Michigan State in the first place.

## TABLE OF CONTENTS

## LIST OF TABLES

## LIST OF FIGURES

## KEY TO ABBREVIATIONS

| | |
|---|---|
| CDR | complementarity-determining region |
| cisA | *cis*-Aconitic anhydride |
| DTT | dithiothreitol |
| EDC | 1-Ethyl-3-(3-dimethylaminopropyl)carbodiimide hydrochloride |
| ELISA | enzyme-linked immunosorbent assay |
| Fab | fragment, antigen-binding |
| Fc | fragment, constant |
| FLAG | DYKDDDDK |
| FTIR | Fourier transform infrared |
| Gly | Glycine |
| HA | hemagglutinin A |
| HER2 | human epidermal growth factor receptor 2 |
| His | polyhistidine |
| HPC | heavy chain protein C |
| IgG | immunoglobulin G |
| K19 | KGSGSGSQLGPYELWELSH |
| kDa | kilodalton |
| KK12 | HWGGWVSGSGKK |
| LBL | layer-by-layer |
| mAbs | monoclonal antibodies |
| MPA | mercaptopropionic acid |

| | |
|---|---|
| MS | mass spectrometry |
| NHS | N-hydroxysuccinimide |
| NT | non-transfected |
| PAA | poly(acrylic acid) |
| PAGE | polyacrylamide gel electrophoresis |
| PBS | phosphate-buffer saline |
| PC | polycarbonate |
| PEI | polyethyleneimine |
| PEM | polyelectrolyte multilayer |
| PT | passed-through |
| RGS2 | regulator G-protein signaling 2 |
| SDS | sodium dodecyl sulfate |
| TSQ | 6-Methoxy-(8-p-toluenesulfonamido)quinoline |
| UV/Vis | ultraviolet/visible |
| VEGF | vascular endothelial growth factor |

# Chapter 1. Introduction

The research in this thesis exploits the specificity of antibody-antigen interactions to create innovative new membrane-based platforms for antibody and protein purification. Membranes functionalized with swellable polyelectrolyte layers offer enhanced capacities compared to traditional membranes modified with affinity molecules, and adsorption of PEMs with readily-functionalized carboxylic acid groups enables high-capacity binding of small synthetic peptides and antibodies. This thesis describes two approaches to antibody purification: 1. Selective purification using a Fab-targeting mimotope and 2. Capture of antibody classes using an Fc-targeting peptide. The two small, immobilized peptides offer similar capacities, which are lower than that of commercial beads but the membrane can more rapidly capture antibodies. In related work, immobilized antibodies effectively isolate specific proteins from complex mixtures. To put this research in context, I first discuss the advantages inherent to membrane-based protein purification (section 1.1), the functionalization of PEMs (section 1.2), antibody purification using small affinity peptides (section 1.3) and protein purification using immobilized antibodies (section 1.4). The end of the introduction presents an outline of this thesis.

## 1.1 Membrane-based protein purification

Development of antibody-based therapies is the fastest growing area of research in the biotechnology industry. In 2014, therapeutic antibodies accounted for 4 of the top 6 biotechnology drugs by revenue in the United States.[1] There are 36 FDA-approved therapeutic antibodies and hundreds more in trials.[2] However, high dosages and treatment frequencies for

therapeutic antibodies necessitate advancements in antibody selection, production and, specifically, purification.[3–5] The industry standard for antibody purification is expensive bead-based affinity adsorption on columns containing immobilized protein A or protein G. Despite the availability of recombinant forms of protein A and protein G, purification costs can amount to over half the total costs of production.[6,7] Due to the slow diffusion of proteins, bead-based methods require relatively long purification times.[8–10]

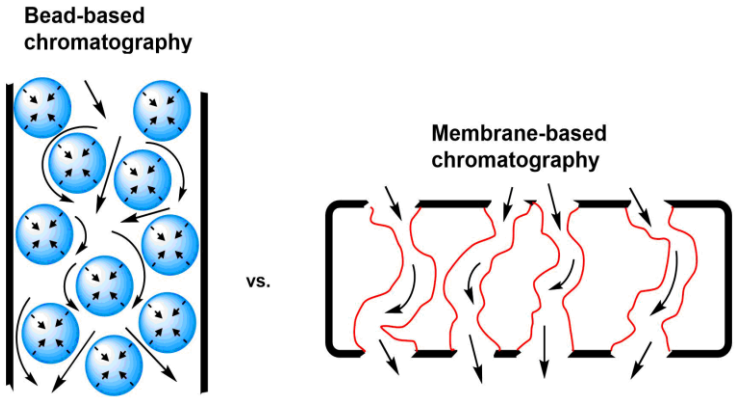


**Figure 1.1**. Illustration of mass transport to binding sites in beads and membranes. The dotted arrows in the blue beads represent slow diffusion into nanopores, whereas the solid arrows denote convection. The red channels are membrane pores trough which solution flows.

As figure 1.1. illustrates, membranes should capture protein more rapidly than bead columns because convection through the membrane pores and short radial diffusion distances facilitate rapid mass transport to binding sites. Nevertheless, the small membrane surface area leads to low capacities relative to traditional bead-based chromatographic methods. To overcome this challenge, several research groups modified membrane pores with highly swollen polymer brushes[11–14] and layer-by-layer (LBL) polyelectrolyte multilayers (PEMs).[15–20] Those studies focused primarily on protein capture via ion-exchange or binding of polyhistidine (His) tags to

metal-ion complexes. This research focuses on modifying swellable PEMs with small peptides and antibodies to rapidly capture proteins for downstream analysis.

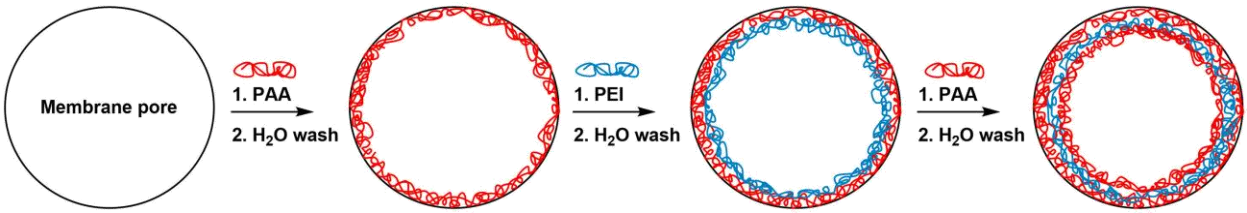


**Figure 1.2.** Layer-by-layer adsorption of PEMs containing alternating poly(acrylic acid) (PAA, red) and polyethyleneimine (PEI, blue) layers.

## 1.2 Functionalizing membranes with derivatizable polyelectrolyte multilayers

Figure 1.2 schematically shows LBL deposition of PEMs in a membrane pore. Alternating adsorption of protonated polyethyleneimine (PEI) and partially protonated poly(acrylic acid) (PAA) leads to a film that swells in water and contains carboxylic acids and primary amine groups that are amenable to additional functionalization.

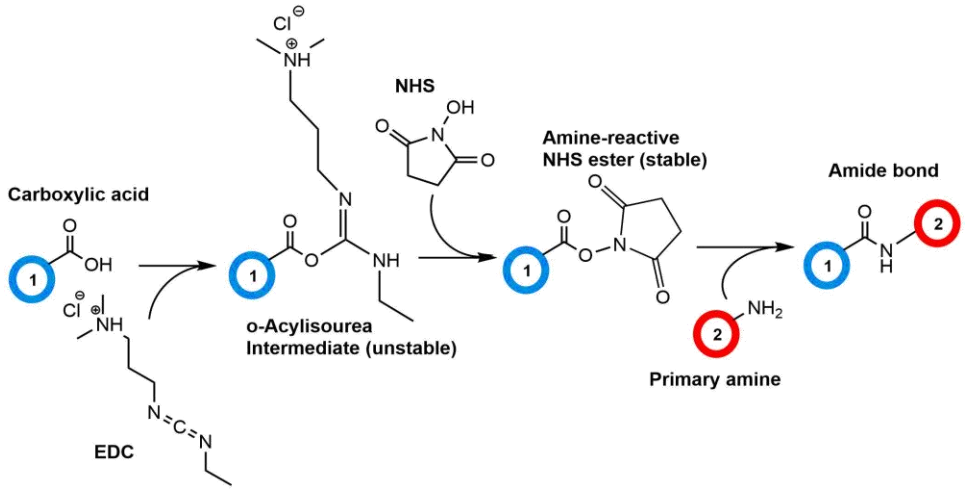


**Figure 1.3.** Mechanism for coupling using EDC and NHS for activation of a carboxylic acid. The reaction performs optimally in aqueous media at pH 4.5-6.0.[21] The blue circles correspond to a molecule containing a carboxylic group, while the red circles correspond to a molecule containing a primary amine.

In particular, we employ 1-ethyl-3-(3-dimethylaminopropyl)carbodiimide hydrochloride (EDC) and N-hydroxysuccinimide (NHS) to activate carboxylic acids for subsequent coupling to molecules, including peptides and proteins containing amine groups.[21–26] Figure 1.3 shows the EDC/NHS coupling mechanism. For coupling reactions involving an immobilized substrate, N-hydroxysuccinimide (NHS) or its sulfonated derivative are often employed to stabilize the reactive carboxyl group.

In my work, a terminal layer of PAA presents carboxylic acid groups for EDC/NHS activation, and for peptide immobilization we purchase peptides with lysine (K) residues at their C-terminus to present primary amines for coupling (see Figure 1.4). Proteins generally present multiple primary amine groups on their surfaces that also couple to a carboxylic acid in this manner. This research will confirm that both peptides and proteins couple to PAA-containing films via EDC/NHS cross-linking.

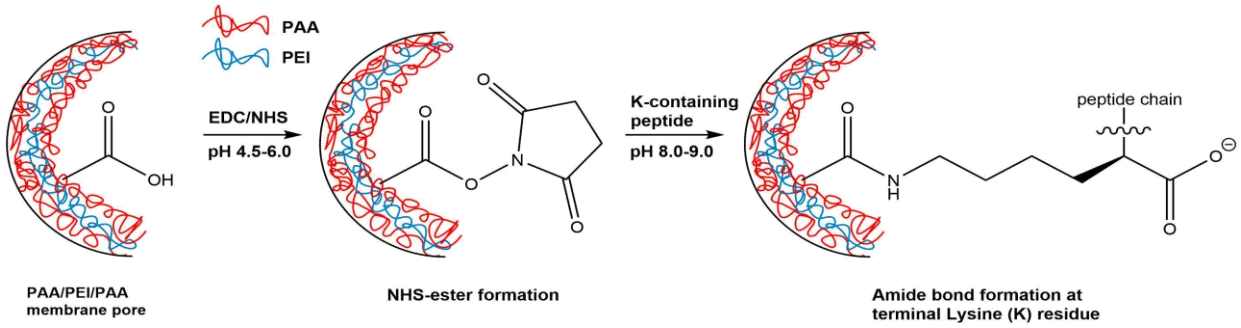


**Figure 1.4.** Peptide/protein immobilization via EDC/NHS mediated coupling. The red layers correspond to PAA, and the blue layer corresponds to PEI. For peptides employed in this research, a terminal Lysine residue couples to PAA carboxyl groups. Proteins present surface amines for the coupling reaction.

## 1.3 Antibody purification using small affinity peptides

In the late 1800s, Paul Ehrlich proposed the antibody-antigen interaction and suggested manipulating such interactions for targeted medicine. He termed this the “magic bullet theory,”

which ultimately led to his 1908 Nobel Prize in Physiology or Medicine.[27–30] During the same period and building on the success of Edward Jenner's smallpox vaccine, Emil Adolf von Behring received the 1901 Nobel Prize in Physiology or Medicine for his work on serum therapy, a predecessor to modern vaccines wherein he injected horses with diphtheria and tetanus toxins, harvested their blood serum and injected humans with the serum at the first sign of symptoms.[31] Although Jenner's work saved millions of lives, it was not exactly the same as the magic bullet that Ehrlich had theorized. Not until Kohler's and Milstein's advent of hybridoma technology in the 1980s could scientists produce and harvest specific antibodies, denoted as monoclonal antibodies (mAbs).[32] With these antibodies in hand, a single medicine could finally target the specific molecule causing an illness. For example, the monoclonal antibody Trastuzumab (Herceptin) has served in breast cancer treatment since its approval in 1998. Herceptin binds to the human epidermal growth factor receptor 2 (HER2) on the tumor cell surface and inhibits tumor metastasis.[33] Nevertheless, producing a monoclonal antibody via hybridoma technology requires a predetermined antibody and a robust purification method.

As mentioned in section 1.1, antibody purification is one of the main costs for production of therapeutic antibodies.[3–7] Although they selectively bind overexpressed antibodies, resins containing either protein A and protein G are expensive and purification may suffer from leaching of fragments during elution and the capture of both active and inactive antibodies.[7,34] Therefore, recent research focused on enhancing antibody purification utilizing bioaffinity ligands,[35,36] synthetic affinity ligands,[37,38] tags,[39,40] and biomimetic peptides.[41,42] In each of these cases, however, the purification method requires a mixture that contains only one monoclonal antibody. Like protein A and protein G, most recently-developed ligands, such as peptides, bind to the fragment, constant (Fc) region of IgG antibodies. (Figure 1.5 illustrates the different

regions of an antibody.) Thus, these ligands discriminate only between antibody isotypes. Applications that require selection of a single antibody to bind a specific epitope require cumbersome methods such as phage display[43] to select high-affinity antibodies from thousands of potential candidates.

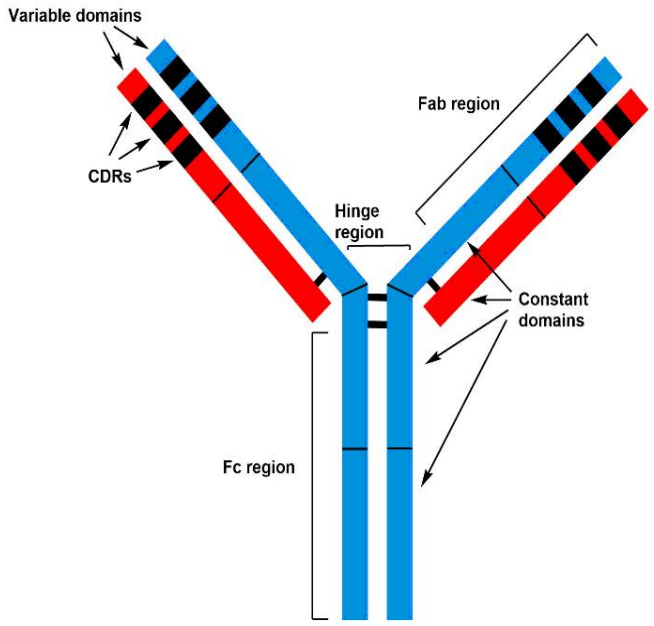


**Figure 1.5.** Antibodies contain two heavy chains (each 50 kDa in mass) and two light chains (each 25 kDa in mass) and are divided into two three regions: the Fc region, two identical Fab regions and the hinge region.[99] The Fc region contains two or three constant domains, whereas each Fab region contains two constant domains and two variable domains.[99] Within each variable domain, three complementarity-determining regions (CDRs) composed of <20 residues each comprise the antigen-binding site.[99]

A small subset of research employed peptide mimotopes in various applications including purification.[44,45] Mimotopes mimic the epitope of a specific antigen and, thus, bind to the fragment, antigen-binding (Fab) region (see Figure 1.5) or paratope of the corresponding antibody. For example, Jiang, *et. al.* isolated the mimotope QLGPYELWELSH via phage display as a HER2–mimetic antigen to the aforementioned Trastuzumab.[46] A synthetic extension of this mimotope (immobilized on a gold substrate through an added cysteine and flexible

spacer) specifically binds Herceptin in the presence of other IgG antibodies for detection in blood serum.[44]

In this research, I investigate two small peptides – one Fc-binding peptide and one Fab-binding peptide – for antibody purification in modified membranes. Yang, *et. al.* identified the Fc-binding peptide via solid-phase hexamer peptide library screening and subsequently confirmed this peptide as a potential alternative to protein A and protein G affinity chromatography.[47,48] The Fab-binding research builds on the recent work by Jiang, *et. al.*[46] and Shang, *et. al.*[44] with the aforementioned HER2-mimicking peptide.

### 1.4 Protein purification using immobilized antibodies

Affinity adsorption is an established method for protein purification. Affinity ligands are either specific or non-specific adsorbers[49] that frequently make use of lectins for glycopeptides and glycoproteins,[50,51] metal ions for Histidine-tagged proteins and phosphopeptides[15,18–20,52,53] and biomimetic dyes for enzymes.[54,55] Immobilized antibodies, however, are perhaps the most specific and most employed ligand in affinity chromatographic platforms for specific protein purification.[56,57] The specificity in the antibody-antigen interaction is attractive for protein purification from complex mixtures.

However, support materials often limit the rate of affinity chromatographic separations. Bead-based and gel-based methods are common, but membranes may enable more rapid protein isolation and enhance control of rinsing to limit non-specific adsorption. Combining the advantages of membranes (see section 1.1) and the specificity of antibody-antigen interactions could yield notable improvements for affinity chromatography. In previous work using adsorbed

PEMs and EDC cross-linking chemistry, Qu, *et. al.*[58,59] found that electrostatic capture of antibodies in membrane yields extensive antibody immobilization but significant leaching in salt solution (Figure 1.6A). In contrast, direct covalent linking of the antibody to the membrane support offered high stability but low capacity (Figure 1.6B). In contrast, a two-step immobilization method, electrostatic capture followed by a covalent linking (Figure 1.6C), preserves both the high capacity of electrostatic immobilization and the stability of covalent binding.[58,60]

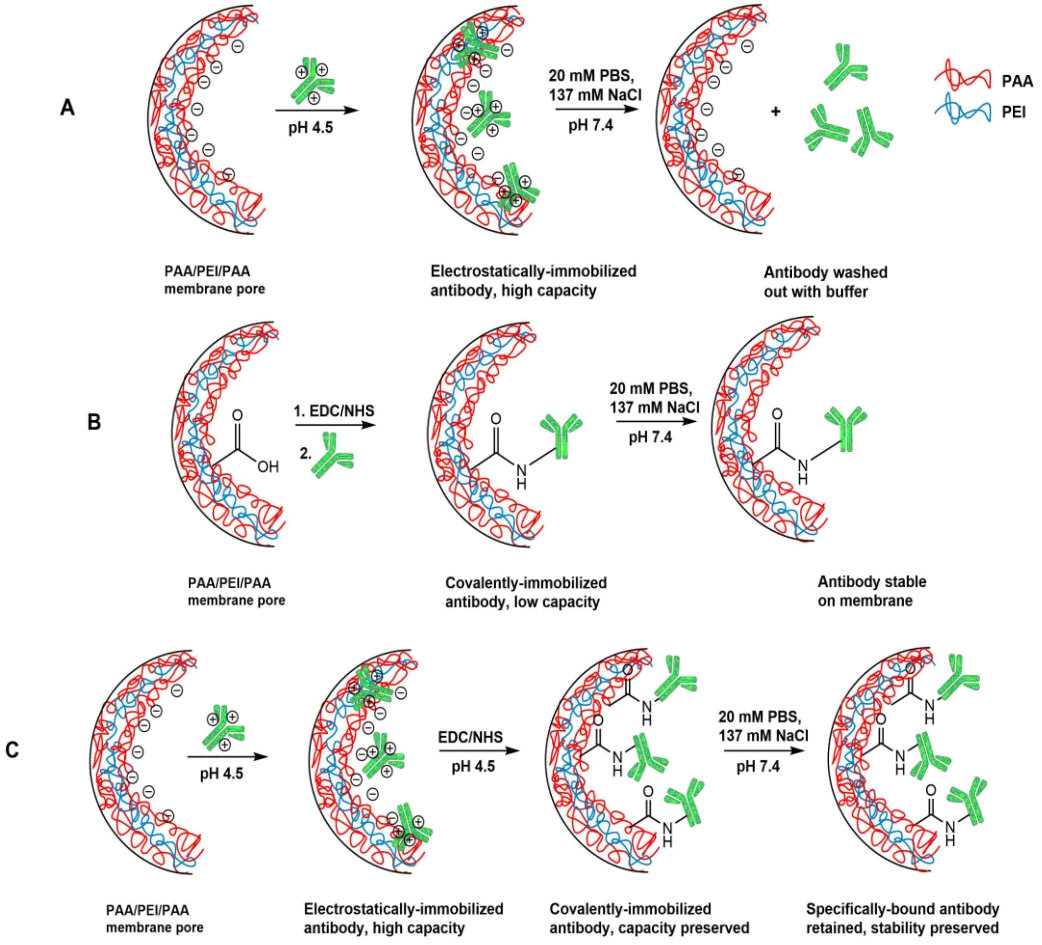


**Figure 1.6.** *[A]* Electrostatic immobilization of antibodies yields high capacity but the antibody elutes from the membrane in salt solutions. *[B]* Direct covalent immobilization does not yield the high capture capacity of electrostatic immobilization, but it does increase the stability of antibody on the membrane. *[C]* The two-step antibody immobilization of antibody first uses electrostatic capture to attain a high capacity, and then covalently links the antibody to the membrane to increase stability.

Affinity tags such as DYKDDDDK (FLAG), polyhistidine and hemagglutinin A (HA).[61] are common targets in antibody-based affinity chromatography. Researchers add these tags via expression vectors that often include other amino acids that enable enzymatic tag removal after purification.[61,62] In collaboration with Dr. Benita Sjogren of the Michigan State University Department of Toxicology and Pharmacology, I examined whether membranes containing anti-hemagglutinin A (anti-HA) antibodies can capture HA-tagged regulator G-protein signaling 2 (HA-RGS2) from cell lysate. RGS2 suppresses breast cancer cell growth[63] and plays key roles in protecting humans against myocardial hypertrophy[64], atrial arrhythmias[65] and hypertension[66]. Sjogren, *et. al.* posit that post-translational modifications may reduce RGS2 activity and subsequently lead to chronic hypertension issues.[66] This research aims to purify HA-RGS2 from cell lysate via membranes containing immobilized anti-HA antibodies. Subsequent rapid in-membrane digestion[67] and phosphopeptide enrichment via $TiO_2$-containing membranes[68] should enable mass spectrometric (MS) analysis phosphorylation.

Immobilized antibodies can also isolate native proteins. In this research, I briefly explore whether an anti-(C-peptide) antibody in a membrane effectively captures C-peptide. C-peptide is a 31 amino acid polypeptide that is co-secreted with insulin from the pancreas and most notably plays a key role in insulin synthesis.[69] Recent research in the Spence group shows that C-peptide, in coordination with $Zn^{2+}$ and albumin, affects ATP release from and glucose uptake into red blood cells.[70,71] Spence, *et. al.* also utilized 3D printing technology to fabricate microfluidic devices that can house small, implantable membranes.[72] A long term goal of this research is to immobilize anti-(C-peptide) antibody into these small, implantable membranes to capture C-peptide in cell excretions as they diffuse across the membrane and into a microfluidic channel.

Such studies may help isolate the specific downstream effects of C-peptide in complex secretions.

### 1.5 Thesis outline

This thesis aims to exploit antibody-antigen interactions in porous membranes to isolate antibodies or their antigens. Utilizing the favorable mass transport phenomena inherent to microporous membranes and the recently-established methods for adsorption and functionalization of PEMs in membranes, this research seeks to improve upon the capacity or throughput of current methods for antibody and protein purification.

In chapter 2, I immobilize small peptides in membranes to capture antibodies. The immobilized species include a highly-specific Fab-binding peptide and an Fc-binding peptide that should capture all IgG antibodies. Fluorescence analyses reveal the extent of peptide immobilization in the membrane, whereas Bradford assays show the extent of subsequent antibody capture. Gel electrophoresis confirms the high purity of antibody eluted from the membrane, and spectroscopy of films on gold wafers demonstrates the effectiveness of different immobilization strategies.

In chapter 3, I discuss the results of antibody immobilization in membranes for tagged-protein and polypeptide capture. Nanodrop UV/Vis analyses confirm antibody immobilization in membrane. Western blot and ELISA analyses demonstrate and quantify the binding capacity for the tagged proteins and polypeptides, whereas I employ gel electrophoresis to assess the purity of tagged eluted from the membrane.

In chapter 4, I draw conclusions from the results presented in chapters 2 and 3 and also discuss future work including preliminary studies on developing an acid-labile linker for universal elution.

REFERENCES

REFERENCES


(1) Morad, R. Top 10 Best-Selling Biotech Drugs http://www.biospace.com/news_story.aspx?StoryID=393360 (accessed Sep 7, 2015).

(2) FDA Approved Antibody-Based Therapeutics http://www.immunologylink.com/FDA-APP-Abs.html (accessed Sep 7, 2015).

(3) Aldington, S.; Bonnerjea, J. Scale-up of Monoclonal Antibody Purification Processes. *J. Chromatogr. B* **2007**, *848* (1), 64–78.

(4) Chames, P.; Van Regenmortel, M.; Weiss, E.; Baty, D. Therapeutic Antibodies: Successes, Limitations and Hopes for the Future. *Br. J. Pharmacol.* **2009**, *157* (2), 220–233.

(5) Thommes, J.; Etzel, M. Alternatives to Chromatographic Separations. *Biotechnol. Prog.* **2007**, *23* (1), 42–45.

(6) Sadana, B. A. M. Efficiency and Economics of Bioseparation: Some Case Studies. *Bioseparation* **1994**, *4* (4), 221–235.

(7) Low, D.; O'Leary, R.; Pujar, N. S. Future of Antibody Purification. *J. Chromatogr. B* **2007**, *848* (1), 48–63.

(8) Zou, H.; Luo, Q.; Zhou, D. Affinity Membrane Chromatography for the Analysis and Purification of Proteins. *J. Biochem. Biophys. Methods* **2001**, *49* (1-3), 199–240.

(9) Boi, C. Membrane Adsorbers as Purification Tools for Monoclonal Antibody Purification. *J. Chromatogr. B. Analyt. Technol. Biomed. Life Sci.* **2007**, *848* (1), 19–27.

(10) Champluvier, B.; Kula, M.-R. Microfiltration Membranes as Pseudo-Affinity Adsorbents: Modification and Comparison with Gel Beads. *J. Chromatogr. A* **1991**, *539* (2), 315–325.

(11) Bhut, B. V; Christensen, K. A.; Husson, S. M. Membrane Chromatography: Protein Purification from E. Coli Lysate Using Newly Designed and Commercial Anion-Exchange Stationary Phases. *J. Chromatogr. A* **2010**, *1217* (30), 4946–4957.

(12) Bhut, B. V.; Wickramasinghe, S. R.; Husson, S. M. Preparation of High-Capacity, Weak Anion-Exchange Membranes for Protein Separations Using Surface-Initiated Atom Transfer Radical Polymerization. *J. Memb. Sci.* **2008**, *325* (1), 176–183.

(13) Bhut, B. V.; Husson, S. M. Dramatic Performance Improvement of Weak Anion-Exchange Membranes for Chromatographic Bioseparations. *J. Memb. Sci.* **2009**, *337* (1-2), 215–223.

(14) Bhut, B. V.; Conrad, K. A.; Husson, S. M. Preparation of High-Performance Membrane Adsorbers by Surface-Initiated AGET ATRP in the Presence of Dissolved Oxygen and Low Catalyst Concentration. *J. Memb. Sci.* **2012**, *390-391*, 43–47.

(15) Bhattacharjee, S.; Dong, J.; Ma, Y.; Hovde, S.; Geiger, J. H.; Baker, G. L.; Bruening, M. L. Formation of High-Capacity Protein-Adsorbing Membranes through Simple

Adsorption of Poly(acrylic Acid)-Containing Films at Low pH. *Langmuir* **2012**, *28* (17), 6885–6892.

(16) Sun, L.; Dai, J.; Baker, G. L.; Bruening, M. L. High-Capacity, Protein-Binding Membranes Based on Polymer Brushes Grown in Porous Substrates. *Chem. Mater.* **2006**, *18*, 4033–4039.

(17) Ning, W.; Bruening, M. L. Rapid Protein Digestion and Purification with Membranes Attached to Pipet Tips. *Anal. Chem.* **2015**, *87* (24), 11984–11989.

(18) Dong, J.; Bruening, M. L. Functionalizing Microporous Membranes for Protein Purification and Protein Digestion. *Annu. Rev. Anal. Chem.* **2015**, *8* (1), 81–100.

(19) Wijeratne, S.; Liu, W.; Dong, J.; Ning, W.; Ratnayake, N. D.; Walker, K. D.; Bruening, M. L. Layer-by-Layer Deposition with Polymers Containing Nitrilotriacetate, A Convenient Route to Fabricate Metal- and Protein-Binding Films. *ACS Appl. Mater. Interfaces* **2016**, *8* (16), 10164–10173.

(20) Ning, W.; Wijeratne, S.; Dong, J.; Bruening, M. L. Immobilization of Carboxymethylated Polyethylenimine-Metal-Ion Complexes in Porous Membranes to Selectively Capture His-Tagged Protein. *ACS Appl. Mater. Interfaces* **2015**, *7* (4), 2575–2584.

(21) Grabarek, Z.; Gergely, J. Zero-Length Crosslinking Procedure with the Use of Active Esters. *Anal. Biochem.* **1990**, *185* (1), 131–135.

(22) Gao, Y.; Kyratzis, I. Covalent Immobilization of Proteins on Carbon Nanotubes Using the Cross-Linker 1-Ethyl-3-(3-Dimethylaminopropyl)carbodiimide--a Critical Assessment. *Bioconjug. Chem.* **2008**, *19* (10), 1945–1950.

(23) Totaro, K. A.; Liao, X.; Bhattacharya, K.; Finneman, J. I.; Sperry, J. B.; Massa, M. A.; Thorn, J.; Ho, S. V; Pentelute, B. L. Systematic Investigation of EDC/sNHS-Mediated Bioconjugation Reactions for Carboxylated Peptide Substrates. *Bioconjug. Chem.* **2016**, *27* (4), 994–1004.

(24) Wang, C.; Yan, Q.; Liu, H.-B.; Zhou, X.-H.; Xiao, S.-J. Different EDC/NHS Activation Mechanisms between PAA and PMAA Brushes and the Following Amidation Reactions. *Langmuir* **2011**, *27* (19), 12058–12068.

(25) Lepvrier, E.; Doigneaux, C.; Moullintraffort, L.; Nazabal, A.; Garnier, C. Optimized Protocol for Protein Macrocomplexes Stabilization Using the EDC, 1-Ethyl-3-(3-(Dimethylamino)propyl)carbodiimide, Zero-Length Cross-Linker. *Anal. Chem.* **2014**, *86* (21), 10524–10530.

(26) Conde, J.; Dias, J. T.; Grazú, V.; Moros, M.; Baptista, P. V; de la Fuente, J. M. Revisiting 30 Years of Biofunctionalization and Surface Chemistry of Inorganic Nanoparticles for Nanomedicine. *Front. Chem.* **2014**, *2* (July), 48.

(27) Ehrlich, P. Die Wertbemessung Des Diphterie-Heilserums Und Deren Theoretische Grundlagen. *Klin. Jahrb.* **1897**, *6*, 299–326.

(28) Ehrlich, P. Croonian Lecture: On Immunity with Special Reference to Cell Life. *Proc. R. Soc. London* **1900**, *66*, 424–448.

(29) Ehrlich, P.; Morganroth, J. Wirkung Und Entstehung Der Aktiven Stoffe Im Serum Nach Der Seiten-Kettentheorie. *Handb. der Pathog. Mikroorganismen* **1904**, *1*, 430–451.

(30) Ehrlich, P.; Morgenroth, J. Die Seitenkettentheorie Der Immunität. *Anleitung zu Hyg. Untersuchungen nach den im Hyg. Inst. der königl. Ludwig-Maximilians-Universität zu München üblichen Methoden zusammengestellt* **1902**, *3*, 381–394.

(31) von Behring, E. A. Serum Therapy in Therapeutics and Medical Science https://www.nobelprize.org/nobel_prizes/medicine/laureates/1901/behring-lecture.html (accessed Sep 7, 2015).

(32) Kohler, G.; Milstein, C. Continuous Cultures of Fused Cells Secreting Antibody of Predefined Specificity. *Nature* **1975**, *256* (5517), 495–497.

(33) Cho, H.-S.; Mason, K.; Ramyar, K. X.; Stanley, A. M.; Gabelli, S. B.; Denney, D. W.; Leahy, D. J. Structure of the Extracellular Region of HER2 Alone and in Complex with the Herceptin Fab. *Nature* **2003**, *421* (12 February 2003), 756–760.

(34) Swinnen, K.; Krul, A.; Van Goidsenhoven, I.; Van Tichelt, N.; Roosen, A.; Van Houdt, K. Performance Comparison of Protein A Affinity Resins for the Purification of Monoclonal Antibodies. *J. Chromatogr. B. Analyt. Technol. Biomed. Life Sci.* **2007**, *848* (1), 97–107.

(35) Huse, K.; Böhme, H.-J.; Scholz, G. H. Purification of Antibodies by Affinity Chromatography. *J. Biochem. Biophys. Methods* **2002**, *51* (3), 217–231.

(36) Roque, A. C. A.; Silva, C. S. O.; Taipa, M. A. Affinity-Based Methodologies and Ligands for Antibody Purification: Advances and Perspectives. *J. Chromatogr. A* **2007**, *1160* (1-2), 44–55.

(37) Barroso, T.; Branco, R. J. F.; Aguiar-Ricardo, A.; Roque, A. C. a. Structural Evaluation of an Alternative Protein A Biomimetic Ligand for Antibody Purification. *J. Comput. Aided. Mol. Des.* **2014**, *28* (1), 25–34.

(38) Barroso, T.; Lourenço, A.; Araújo, M.; Bonifácio, V. D. B.; Roque, A. C. a; Aguiar-Ricardo, A. A Green Approach toward Antibody Purification: A Sustainable Biomimetic Ligand for Direct Immobilization on (Bio)polymeric Supports. *J. Mol. Recognit.* **2013**, *26*, 662–671.

(39) Lesley, S. A.; Groskreutz, D. J. Simple Affinity Purification of Antibodies Using in Vivo Biotinylation of a Fusion Protein. *J. Immunol. Methods* **1997**, *207* (2), 147–155.

(40) Sun, L.; Ghosh, I.; Xu, M.-Q. Generation of an Affinity Column for Antibody Purification by Intein-Mediated Protein Ligation. *J. Immunol. Methods* **2003**, *282* (1-2), 45–52.

(41) Alves, N. J.; Stimple, S. D.; Handlogten, M. W.; Ashley, J. D.; Kiziltepe, T.; Bilgicer, B. Small-Molecule-Based Affinity Chromatography Method for Antibody Purification via Nucleotide Binding Site Targeting. *Anal. Chem.* **2012**, *84*, 7721–7728.

(42) Verdoliva, A.; Pannone, F.; Rossi, M.; Catello, S.; Manfredi, V. Affinity Purification of Polyclonal Antibodies Using a New All-D Synthetic Peptide Ligand: Comparison with Protein A and Protein G. *J. Immunol. Methods* **2002**, *271* (1-2), 77–88.

(43) Smith, G. P.; Petrenko, V. A. Phage Display. *Chem. Rev.* **1997**, *97* (2), 391–410.

(44) Shang, Y.; Singh, P. R.; Chisti, M. M.; Mernaugh, R.; Zeng, X. Immobilization of a Human Epidermal Growth Factor Receptor 2 Mimotope-Derived Synthetic Peptide on Au and Its Potential Application for Detection of Herceptin in Human Serum by Quartz Crystal Microbalance. *Anal. Chem.* **2011**, *83*, 8928–8936.

(45) Leo, N.; Shang, Y.; Yu, J.; Zeng, X. Characterization of Self-Assembled Monolayers of Peptide Mimotopes of CD20 Antigen and Their Binding with Rituximab. *Langmuir* **2015**, *31* (51), 13764–13772.

(46) Jiang, B.; Liu, W.; Qu, H.; Meng, L.; Song, S.; Ouyang, T.; Shou, C. A Novel Peptide Isolated from a Phage Display Peptide Library with Trastuzumab Can Mimic Antigen Epitope of HER-2. *J. Biol. Chem.* **2005**, *280* (6), 4656–4662.

(47) Yang, H.; Gurgel, P. V.; Carbonell, R. G. Purification of Human Immunoglobulin G via Fc-Specific Small Peptide Ligand Affinity Chromatography. *J. Chromatogr. A* **2009**, *1216* (6), 910–918.

(48) Yang, H.; Gurgel, P. V.; Carbonell, R. G. Hexamer Peptide Affinity Resins That Bind the Fc Region of Human Immunoglobulin G. *J. Pept. Res.* **2008**, *66*, 120–137.

(49) Walters, R. R. Affinity Chromatography. *Anal. Chem.* **1985**, *57* (11), 1099A – 1114A.

(50) Ghosh, D.; Krokhin, O.; Antonovici, M.; Ens, W.; Standing, K. G.; Beavis, R. C.; Wilkins, J. A. Lectin Affinity as an Approach to the Proteomic Analysis of Membrane Glycoproteins. *J. Proteome Res.* **2004**, *3* (4), 841–850.

(51) Kubota, K.; Sato, Y.; Suzuki, Y.; Goto-Inoue, N.; Toda, T.; Suzuki, M.; Hisanaga, S.; Suzuki, A.; Endo, T. Analysis of Glycopeptides Using Lectin Affinity Chromatography with MALDI-TOF Mass Spectrometry. *Anal. Chem.* **2008**, *80* (10), 3693–3698.

(52) Porath, J.; Carlsson, J.; Olsson, I.; Belfrage, G. Metal Chelate Affinity Chromatography, a New Approach to Protein Fractionation. *Nature* **1975**, *258* (5536), 598–599.

(53) Porath, J. Immobilized Metal Ion Affinity Chromatography. *Protein Expr. Purif.* **1992**, *3* (4), 263–281.

(54) Dean, P. D. G.; Watson, D. H. Protein Purification Using Immobilised Triazine Dyes. *J. Chromatogr. A* **1979**, *165* (3), 301–319.

(55) Clonis, Y. .; Labrou, N. .; Kotsira, V. P.; Mazitsos, C.; Melissis, S.; Gogolas, G. Biomimetic Dyes as Affinity Chromatography Tools in Enzyme Purification. *J. Chromatogr. A* **2000**, *891* (1), 33–44.

(56) Schneider, C.; Newman, R.; Sutherland, D.; Asser, U.; Greaves, M. A One-Step Purification of Membrane Proteins Using a High Efficiency Immunomatrix. *J. Biol. Chem.* **1982**, *257* (18), 10766–10769.

(57) Cuatrecasas, P. Protein Purification by Affinity Chromatography. *J. Biochem. Biophys. Methods* **1970**, *245* (12), 3059–3065.

(58) Dong, J. Functionalized Porous Membranes for Rapid Protein Purification and Controlled Protein Digestion Prior to Mass Spectrometry Analysis, Ph.D. Dissertation, Michigan State University, 2014.

(59) Qu, Z.; Chen, K.; Gu, H.; Xu, H. Covalent Immobilization of Proteins on 3D Poly(acrylic Acid) Brushes: Mechanism Study and a More Effective and Controllable Process. *Bioconjug. Chem.* **2014**, *25* (2), 370–378.

(60) Jain, P.; Vyas, M. K.; Geiger, J. H.; Baker, G. L.; Bruening, M. L. Protein Purification with Polymeric Affinity Membranes Containing Functionalized Poly(acid) Brushes. *Biomacromolecules* **2010**, *11* (4), 1019–1026.

(61) Lichty, J. J.; Malecki, J. L.; Agnew, H. D.; Michelson-Horowitz, D. J.; Tan, S. Comparison of Affinity Tags for Protein Purification. *Protein Expr. Purif.* **2005**, *41* (1), 98–105.

(62) Terpe, K. Overview of Bacterial Expression Systems for Heterologous Protein Production: From Molecular and Biochemical Fundamentals to Commercial Systems. *Appl. Microbiol. Biotechnol.* **2006**, *72* (2), 211–222.

(63) Lyu, J. H.; Park, D. W.; Huang, B.; Kang, S. H.; Lee, S. J.; Lee, C.; Bae, Y. S.; Lee, J. G.; Baek, S. H. RGS2 Suppresses Breast Cancer Cell Growth via a MCPIP1-Dependent Pathway. *J. Cell. Biochem.* **2015**, *116* (2), 260–267.

(64) Nunn, C.; Zou, M.-X.; Sobiesiak, A. J.; Roy, A. A.; Kirshenbaum, L. A.; Chidiac, P. RGS2 Inhibits Beta-Adrenergic Receptor-Induced Cardiomyocyte Hypertrophy. *Cell. Signal.* **2010**, *22* (8), 1231–1239.

(65) Tuomi, J. M.; Chidiac, P.; Jones, D. L. Evidence for Enhanced M3 Muscarinic Receptor Function and Sensitivity to Atrial Arrhythmia in the RGS2-Deficient Mouse. *Am. J. Physiol. Heart Circ. Physiol.* **2010**, *298* (2), H554–H561.

(66) Raveh, A.; Schultz, P. J.; Aschermann, L.; Carpenter, C.; Tamayo-Castillo, G.; Cao, S.; Clardy, J.; Neubig, R. R.; Sherman, D. H.; Sjogren, B. Identification of Protein Kinase C Activation as a Novel Mechanism for RGS2 Protein Upregulation through Phenotypic Screening of Natural Product Extracts. *Mol. Pharmacol.* **2014**, *86* (4), 406–416.

(67) Tan, Y. J.; Wang, W. H.; Zheng, Y.; Dong, J.; Stefano, G.; Brandizzi, F.; Garavito, R. M.; Reid, G. E.; Bruening, M. L. Limited Proteolysis via Millisecond Digestions in Protease-Modified Membranes. *Anal. Chem.* **2012**, *84* (19), 8357–8363.

(68) Tan, Y. J.; Sui, D.; Wang, W. H.; Kuo, M. H.; Reid, G. E.; Bruening, M. L. Phosphopeptide Enrichment with TiO2-Modified Membranes and Investigation of Tau Protein Phosphorylation. *Anal. Chem.* **2013**, *85* (12), 5699–5706.

(69) Steiner, D. F.; Cunningham, D.; Spigelman, L.; Aten, B. Insulin Biosynthesis: Evidence for a Precursor. *Science* **1967**, *157* (3789), 697–700.

(70) Meyer, J. A.; Froelich, J. M.; Reid, G. E.; Karunarathne, W. K. A.; Spence, D. M. Metal-Activated C-Peptide Facilitates Glucose Clearance and the Release of a Nitric Oxide Stimulus via the GLUT1 Transporter. *Diabetologia* **2008**, *51* (1), 175–182.

(71) Liu, Y.; Chen, C.; Summers, S.; Medawala, W.; Spence, D. M. C-Peptide and Zinc Delivery to Erythrocytes Requires the Presence of Albumin: Implications in Diabetes Explored with a 3D-Printed Fluidic Device. *Integr. Biol.* **2015**, *7* (5), 534–543.

(72) Lockwood, S. Y.; Meisel, J. E.; Monsma, F. J.; Spence, D. M. A Diffusion-Based and Dynamic 3D-Printed Device That Enables Parallel in Vitro Pharmacokinetic Profiling of Molecules. *Anal. Chem.* **2016**, *88* (3), 1864–1870.

(73) Kim, K. J.; Li, B.; Houck, K.; Winer, J.; Ferrara, N. The Vascular Endothelial Growth Factor Proteins: Identification of Biologically Relevant Regions by Neutralizing Monoclonal Antibodies. *Growth Factors* **1992**, *7* (1), 53–64.

(74) Presta, L. G.; Chen, H.; O'Connor, S. J.; Chisholm, V.; Meng, Y. G.; Krummen, L.; Winkler, M.; Ferrara, N. Humanization of an Anti-Vascular Endothelial Growth Factor Monoclonal Antibody for the Therapy of Solid Tumors and Other Disorders. *Cancer Res.* **1997**, *57* (20), 4593–4599.

(75) Tsai, C. W.; Jheng, S. L.; Chen, W. Y.; Ruaan, R. C. Strategy of Fc-Recognizable Peptide Ligand Design for Oriented Immobilization of Antibody. *Anal. Chem.* **2014**, *86* (6), 2931–2938.

(76) Jeong, Y. jin; Kang, H. J.; Bae, K. H.; Kim, M. G.; Chung, S. J. Efficient Selection of IgG Fc Domain-Binding Peptides Fused to Fluorescent Protein Using E. Coli Expression System and Dot-Blotting Assay. *Peptides* **2010**, *31* (2), 202–206.

(77) Sugita, T.; Katayama, M.; Okochi, M.; Kato, R.; Ichihara, T.; Honda, H. Screening of Peptide Ligands That Bind to the Fc Region of IgG Using Peptide Array and Its Application to Affinity Purification of Antibody. *Biochem. Eng. J.* **2013**, *79*, 33–40.

(78) Zhao, W. W.; Shi, Q. H.; Sun, Y. FYWHCLDE-Based Affinity Chromatography of IgG: Effect of Ligand Density and Purifications of Human IgG and Monoclonal Antibody. *J. Chromatogr. A* **2014**, *1355*, 107–114.

(79) Wei, Y.; Xu, J.; Zhang, L.; Fu, Y.; Xu, X. Development of Novel Small Peptide Ligands for Antibody Purification. *RSC Adv.* **2015**, *5* (82), 67093–67101.

(80) Lund, L. N.; Gustavsson, P. E.; Michael, R.; Lindgren, J.; Nørskov-Lauritsen, L.; Lund, M.; Houen, G.; Staby, A.; St. Hilaire, P. M. Novel Peptide Ligand with High Binding Capacity for Antibody Purification. *J. Chromatogr. A* **2012**, *1225*, 158–167.

(81) Datta, S.; Cecil, C.; Bhattacharyya, D. Functionalized Membranes by Layer-By-Layer Assembly of Polyelectrolytes and In Situ Polymerization of Acrylic Acid for Applications in Enzymatic Catalysis. *Ind. Eng. Chem. Res.* **2008**, *47* (14), 4586–4597.

(82) Sousa, M. M.; Steen, K. W.; Hagen, L.; Slupphaug, G. Antibody Cross-Linking and Target Elution Protocols Used for Immunoprecipitation Significantly Modulate Signal-to Noise Ratio in Downstream 2D-PAGE Analysis. *Proteome Sci.* **2011**, *9* (1), 45.

(83) Conley, R. T. Interpretation of Infrared Spectra, Part II: Common Functional Groups. In *Infrared Spectroscopy*; Allyn and Bacon, Inc.: Boston, MA, 1966; pp 110–175.

(84) Fox, J. L.; Stevens, S. E.; Taylor, C. P.; Poulsen, L. L. SDS Removal from Protein by

Polystyrene Beads. *Anal. Biochem.* **1978**, *87* (1), 253–256.

(85) Puchades, M.; Westman, A.; Blennow, K.; Davidsson, P. Removal of Sodium Dodecyl Sulfate from Protein Samples prior to Matrix-Assisted Laser Desorption/ionization Mass Spectrometry. *Rapid Commun. Mass Spectrom.* **1999**, *13* (5), 344–349.

(86) Bruening, M. L.; Dotzauer, D. M.; Jain, P.; Ouyang, L.; Baker, G. L. Creation of Functional Membranes Using Polyelectrolyte Multilayers and Polymer Brushes. *Langmuir* **2008**, *24* (15), 7663–7673.

(87) Huang, W.; Kim, J. B.; Bruening, M. L.; Baker, G. L. Functionalization of Surfaces by Water-Accelerated Atom-Transfer Radical Polymerization of Hydroxyethyl Methacrylate and Subsequent Derivatization. *Macromolecules* **2002**, *35* (4), 1175–1179.

(88) Dai, J.; Bao, Z.; Sun, L.; Hong, S. U.; Baker, G. L.; Bruening, M. L. High-Capacity Binding of Proteins by Poly(acrylic Acid) Brushes and Their Derivatives. *Langmuir* **2006**, *22* (9), 4274–4281.

(89) Dai, J.; Baker, G. L.; Bruening, M. L. Use of Porous Membranes Modified with Polyelectrolyte Multilayers as Substrates for Protein Arrays with Low Nonspecific Adsorption. *Anal. Chem.* **2006**, *78* (1), 135–140.

(90) Waugh, D. S. Making the Most of Affinity Tags. *Trends Biotechnol.* **2005**, *23* (6), 316–320.

(91) Young, C. L.; Britton, Z. T.; Robinson, A. S. Recombinant Protein Expression and Purification: A Comprehensive Review of Affinity Tags and Microbial Applications. *Biotechnol. J.* **2012**, *7* (5), 620–634.

(92) Arnau, J.; Lauritzen, C.; Petersen, G. E.; Pedersen, J. Current Strategies for the Use of Affinity Tags and Tag Removal for the Purification of Recombinant Proteins. *Protein Expr. Purif.* **2006**, *48* (1), 1–13.

(93) Ghosh, R. Protein Separation Using Membrane Chromatography: Opportunities and Challenges. *J. Chromatogr. A* **2002**, *952* (1-2), 13–27.

(94) Rigaud, J. L.; Levy, D.; Mosser, G.; Lambert, O. Detergent Removal by Non-Polar Polystyrene Beads: Applications to Membrane Protein Reconstitution and Two-Dimensional Crystallization. *Eur. Biophys. J.* **1998**, *27* (4), 305–319.

(95) Battogtokh, G.; Ko, Y. T. Active-Targeted pH-Responsive Albumin–photosensitizer Conjugate Nanoparticles as Theranostic Agents. *J. Mater. Chem. B* **2015**, *3* (48), 9349–9359.

(96) Bonifacino, J. S.; Dell'Angelica, E. C.; Springer, T. A. Immunoprecipitation. In *Current Protocols in Immunology*; John Wiley & Sons, Inc., 2001; pp 8.3.1–8.3.28.

(97) Otto, J. J.; Lee, S. W. Immunoprecipitation Methods. *Methods Cell Biol.* **1993**, *37*, 119–127.

(98) Kessler, S. W. *Immunochemical Techniques: Part B*; Methods in Enzymology; Elsevier, 1981; Vol. 73, pp. 442-459.

(99) Charles A Janeway, J.; Travers, P.; Walport, M.; Shlomchik, M. J. *Immunobiology*; Garland Science: New York, New York, 2001.

*Parts of this chapter are adapted from a working manuscript to be submitted in 2016. The Fab-binding peptide work was conducted in coordination with and at the direction of Wenjing Ning of the Bruening Research Group.*

# Chapter 2. Membrane-bound synthetic peptides for antibody purification and detection

## 2.1 Introduction

Because of their high specificity, monoclonal antibodies are becoming the therapy of choice for cancer treatment. The monoclonal antibody Trastuzumab (Herceptin) binds specifically to the human epidermal growth factor receptor 2 (HER2) on the tumor cell surface and inhibits tumor metastasis (see section 1.3).[1] Bevacizumab (Avastin), another therapeutic monoclonal antibody, binds to the vascular endothelial growth factor (VEGF), a major mediator of angiogenesis and growth.[2,3] Although therapeutic monoclonal antibodies are remarkably effective, their production and purification are very expensive.[4,5] In some cases, purification accounts for 80% of the manufacturing cost.[6] Thus, alternative purification methods are vital to reducing the costs of these live-saving treatments.

Columns containing protein A and protein G selectively bind to the Fc region of IgG antibodies to isolate them from bacteria lysates. However, even recombinant forms of protein A and protein G contribute significantly to the cost of producing monoclonal antibodies.[6,7] In the search for other molecules that selectively capture antibodies, several studies identified small Fc-binding peptides.[8-14] Small peptides are an alternative to protein A and protein G because of their potentially lower cost of production and greater binding capacity. Fc-binding peptides and

proteins, however, discriminate only between isotypes and necessitate cumbersome methods such as phage display and hybridoma technology to select specific high-affinity monoclonal antibodies for production. Furthermore, Fc-binding ligands will not bind a specific antibody in blood due to the presence of other IgG antibodies. Rapid, inexpensive quantitation of therapeutic antibodies in blood is crucial for understanding how antibody clearance varies from patient to patient and may enable more individualized treatments.

Mimotopes mimic the antigenic complement to a specific antibody and, therefore, bind to the Fab region,[15-17] which enables them to discriminate between active and inactive antibodies as well as between different antibodies of the same isotype. Thus, immobilization of Fab-binding peptides in porous membranes should allow capture of specific antibodies in matrices such as blood serum (Figure 2.1).

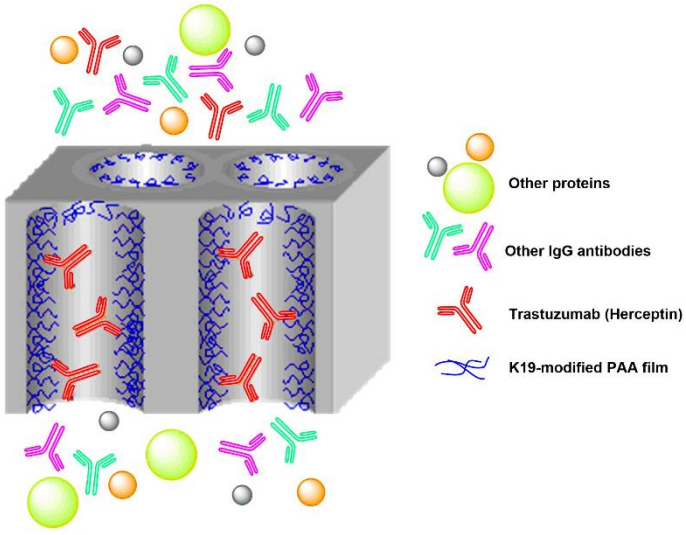


**Figure 2.1.** Illustration of selective Herceptin capture in membranes modified with the K19 peptide. K19 selectively binds Herceptin in the presence of other IgG antibodies.

This study examines monoclonal antibody purification with both an Fc-binding peptide and a more specific, Fab-binding peptide immobilized in porous membranes. We aim to develop

rapid antibody purification and detection methods that exploit rapid convective mass transport to binding sites to facilitate antibody purification in minutes. We selected HWGWV as an Fc-binding sequence based on its 2 fluorescent tryptophan residues and reported capture of IgG with high purity and capacity.[11] To immobilize the peptide in membranes, we added a flexible 4 amino acid spacer arm (SGSG) and 2 lysine residues to the C-terminus for a final peptide sequence of HWGGWVSGSGKK – referred to as KK12 in this thesis. The Fab-binding peptide, KGSGSGSQLGPYELWELSH – denoted here as K19 – is similar to a peptide that Zeng, *et. al.*[16] used to specifically capture Herceptin on a quartz crystal microbalance. We replaced the N-terminal cysteine with a lysine residue to enable the immobilization through an amide linkage via EDC/NHS chemistry. Based on changes in the fluorescence of peptide loading solutions after circulation through the membrane, we determined the peptide loading in membranes, and similarly Bradford assays revealed the binding capacities for Herceptin and Avastin on both KK12- and K19-modified membranes. This study examines the reusability of the KK12-modified membranes as well as selective purification of Herceptin from human blood serum.

## 2.2 Experimental

### 2.2.1 Materials

Sheets of hydroxylated nylon membranes (LoProdyne® LP, pore size=1.2 μm, thickness=110 μm, 50% porosity) were obtained from Pall Corporation and cut into 25 mm disks. Au-coated silicon wafers (200 nm sputtered Au on 20 nm Cr on Si) were obtained from Addison. Poly(acrylic acid) (PAA, $M_w$=100,000 Da, 35% in water) was obtained from Sigma-Aldrich and branched polyethyleneimine (PEI, $M_w$=250,000 Da) was purchased from Aldrich. Aqueous solutions of 0.01 M PAA (repeating unit concentration in 0.5 M NaCl, pH 3) and 2.0

mg/mL PEI (pH 3) were prepared in deionized water (18.2 MΩcm, Milli-Q), and the pH values of the solutions were adjusted by adding 0.1 M HCl or 0.1 M NaOH dropwise. 1-Ethyl-3-(3-dimethylaminopropyl)carbodiimide hydrochloride (EDC) and N-hydroxysuccinimide (NHS) were purchased from Sigma-Aldrich. Custom peptides K19 (95% purity, 2 mg vials) and KK12 (95% purity, 2 mg vials) were purchased from Selleck Chemicals. The antibodies Herceptin (Trastuzumab, 21 mg/mL, Genentech) and Avastin (Bevacizumab, 25 mg/mL, Genentech) were obtained from Dr. Mohammad Christi (Oakland University/Michigan State University, Bloomfield Hills Oncology). Human serum (from human male AB plasma) was purchased from Sigma-Aldrich. Coomassie protein assay reagent (Blue G250-based reagent) was purchased from Thermo Scientific.

### 2.2.2 Preparation of polyelectrolyte multilayers

Polyelectrolyte layers were deposited according to a literature protocol.[18,19] Nylon membranes (0.0346 $cm^3$ vol.) were first cleaned in a UV/$O_3$ chamber (Boekel UV Clean, #135500) for 15 minutes, placed in a homemade Teflon holder (3.14 $cm^2$ exposed external surface area) and rinsed with deionized water for 10 minutes. Ten mL of 0.01 M PAA (0.5 M NaCl, pH 3) was circulated through the membrane at a flow rate of 1 mL/min for 30 minutes using a peristaltic pump (Cole-Parmer Masterflex C/L) and the membrane was rinsed with deionized water for 10 minutes. Subsequent layers of PEI and PAA were deposited similarly. After adsorption of the terminal PAA layer, the membrane was rinsed with deionized water for 10 minutes.

Au-coated silicon wafers were cut into 24 x 11 mm rectangles, cleaned in a UV/$O_3$ chamber for 15 minutes and rinsed with ethanol. The wafers were then placed in a 5 mM

mercaptopropionic acid (MPA) solution overnight to allow the assembly and organization of the MPA monolayer, which provides a negatively-charged surface a neutral pH. The wafer was subsequently rinsed with ethanol and then deionized water before drying with $N_2$. To deposit the polyelectrolyte layers, the wafers were exposed to 5 mL of 2.0 mg/mL PEI (pH 3) solution for 30 minutes, rinsed with deionized water and dried with $N_2$. Subsequent layers of PAA and PEI were adsorbed similarly. Polyelectrolyte film deposition was confirmed via reflectance FTIR (Thermo Scientific, Nicolet 6700 FTIR spectrometer, Pike grazing angle 80° holder).

### 2.2.3 Covalent immobilization of synthetic peptides

After deposition of PAA/PEI/PAA films in the manner PAA/PEI/PAA, 5 mL of aqueous 0.1 M EDC/NHS was circulated through the membrane for 1 hour at a flow rate of 1.0 mL/min. A 1 mg/mL peptide solution (K19 or KK12) was obtained by dissolving 2 mg of peptide in 2 mL of water, and the pH of this solution was adjusted to 8-9 by dropwise addition of 0.1 M NaOH. The peptide solution was circulated through the activated membrane for 2 h, and the membrane was subsequently washed with deionized water for 10 minutes. The peptide solutions were analyzed via fluorescence spectroscopy (Molecular Devices SpectraMax m5) before and after circulation through the membrane to determine the amount of immobilized peptide. A 100 μL aliquot of the feed solution was set aside and diluted to 0.1 mM. Fluorescence standards of 0.5, 1.0, 2.0, 5.0, 10.0 15.0 and 20.0 μM peptide were prepared from the 0.1 mM stock solution, and prior to analysis the solution employed to load the membrane was diluted in the same manner as the 20 μM standard. The excitation wavelength was 280 nm, and emission spectra from 300-400 nm were collected for each standard and the diluted loading solutions. Emission intensities at the

spectral maximum (355 nm for K19, 350 nm for KK12) were used to plot the calibration curve and calculate peptide capacity.

MPA monolayers and $(PEI/PAA)_2$ polyelectrolyte films were first prepared on Au-coated Si wafers. The wafers were likewise immersed in 5 mL of aqueous 0.1 M EDC/NHS for 1 h and subsequently rinsed with deionized water, dried with $N_2$ and analyzed via reflectance FTIR to confirm successful activation of -COOH groups. The activated wafers were then immersed in an aqueous 1 mg/mL peptide solution for 2 h. The wafers were rinsed and dried as before and analyzed via reflectance FTIR spectroscopy to confirm peptide immobilization.

### 2.2.4 Antibody capture and elution in peptide-modified membranes

KK12-modified membranes were first washed with 5 mL of 20 mM phosphate-buffered saline (PBS) (no added NaCl, pH 7.4). Avastin was diluted from the stock solution to 1 mg/mL and subsequently to 0.1 mg/mL in 20 mM PBS (no added NaCl, pH 7.4). Ten mL of this diluted Avastin solutions was passed through the membrane at a flow rate of 0.5 mL/min, and the membrane was subsequently washed with 1 mL aliquots of 20 mM PBS containing 137 mM NaCl (pH 7.4) and 20 mM PBS containing 500 mM NaCl (pH 7.4). Avastin was eluted from the membrane with 100 mM Glycine (pH 2.7). The binding capacity of both Avastin and Herceptin on the KK12-modified membranes were determined via breakthrough curves using Bradford assay. Standards containing of 0.02, 0.04, 0.06, 0.08 and 0.10 mg/mL antibody were obtained via dilution from the stock solution and used to prepare a calibration curve.

To assess the reusability of KK12-modified membranes, after Avastin capture and elution, the membrane was washed with deionized water and 10 mL of 20 mM PBS buffer (no

NaCl, pH 7.4), and another 10 mL of Avastin solution was passed through the membrane according to the protocol above. The binding capacity was again determined via a breakthrough curve obtained using a Bradford assay.

KK12-modified wafers were immersed in 0.1 mg/mL Herceptin in 20 mM PBS (no NaCl, pH 7.4) for 1 h and subsequently rinsed with 20 mM PBS (137 mM NaCl, pH 7.4) and deionized water. Herceptin capture was confirmed via reflectance FTIR. To elute Herceptin, the wafers were then exposed to 100 mM Glycine (pH 2.7) for 30 minutes and subsequently rinsed with deionized water. Herceptin elution was confirmed via reflectance FTIR spectroscopy. Binding of Avastin to KK12-modified wafers (or lack of binding) was evaluated in the same manner.

K19-modified membranes were first washed with 5 mL of 20 mM PBS (137 mM NaCl, pH 7.4). Herceptin was diluted from the stock solution to 1 mg/mL and subsequently to 0.1 mg/mL in 20 mM PBS (137 mM NaCl, pH 7.4). Ten mL of the diluted solution was passed through the membrane at a flow rate of 0.5 mL/min. The membrane was subsequently washed with 1 mL aliquots of 20 mM PBS (137 mM NaCl, pH 7.4) and 20 mM PBS (500 mM NaCl, pH 7.4). Herceptin was eluted from the membrane with 2% sodium dodecyl sulfate (SDS) containing 100 mM dithiothreitol (DTT) according to literature conditions.[20] The binding capacities for Herceptin and Avastin on the K19-modified membranes were determined via breakthrough curves obtained using Bradford assays. Herceptin binding capacities were determined on membranes with exposed diameters of 2.5 cm and 1.0 cm (0.0346 $cm^3$ and 0.00864 $cm^3$, respectively), and Avastin binding capacities were only determined using a 2.5 cm diameter membrane. Because SDS is incompatible with the Coomassie protein assay reagent, the

presence of Herceptin in a 150 μL elution was confirmed via sodium dodecyl sulfate polyacrylamide gel electrophoresis (SDS-PAGE).

As with KK12-modified wafers, the K19-modified wafers were immersed in 0.1 mg/mL Herceptin in 20 mM PBS (137 mM NaCl, pH 7.4) for 1 hour and subsequently rinsed with 20 mM PBS (137 mM NaCl, pH 7.4) and deionized water. Herceptin capture was confirmed via reflectance FTIR spectroscopy. The Herceptin-capture wafers were then immersed in 10 mL of 2% SDS (100 mM DTT) for 30 minutes and subsequently rinsed with deionized water. Reflectance FTIR spectroscopy confirmed the removal of Herceptin. Binding of Avastin to K19-modified wafers (or lack of binding) was evaluated similarly.

### 2.2.5 Purification of Herceptin from human serum

Human serum was diluted 1:3 in 20 mM PBS (137 mM NaCl, pH 7.4) and spiked with Herceptin to achieve a Herceptin concentration of 0.1 mg/mL. One mL of the spiked solution was circulated through membrane (1.0 cm diameter, 0.00864 $cm^3$ vol.) for 30 minutes, and the membrane was subsequently washed with 1 mL aliquots of 20 mM PBS (137 mM NaCl, pH 7.4) and 20 mM PBS (500 mM NaCl, pH 7.4). Herceptin was eluted from the membrane with 150 μL 2% SDS (100 mM DTT). The purity of Herceptin in the elution was determined via SDS-PAGE.

## 2.3 Results and discussion

### 2.3.1 Verification of peptide immobilization

Using reflectance FTIR spectroscopy, we first investigated peptide anchoring to $(PEI/PAA)_2$ films on Au-coated Si wafers (see Figure 2.2). IR spectra after deposition of a MPA monolayer and a $(PEI/PAA)_2$ film show a dominant acid carbonyl peak at 1710 $cm^{-1}$. Upon activation with EDC/NHS, the spectra of the films contain succinimide ester bands centered at 1800 $cm^{-1}$ and 1770 $cm^{-1}$ along with a succinimide asymmetric stretch centered at 1743 $cm^{-1}$.[21] After immersion in the peptide solution and rinsing, amide I and amide II bands appear around 1660 $cm^{-1}$ and 1560 $cm^{-1}$, respectively, confirming peptide immobilization. However, the amide bands are much larger for KK12 than for K19, suggesting more immobilization of the smaller peptide with 2 lysine residues.

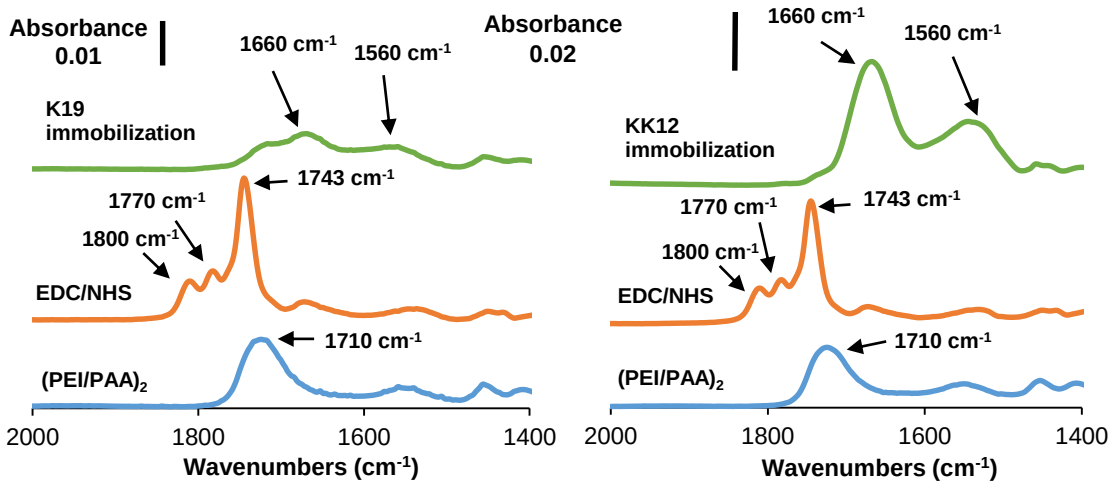


**Figure 2.2.** Reflectance FTIR spectra of $(PEI/PAA)_2$ films on Au-coated Si wafers before and after activation with EDC/NHS solution and after subsequent immobilization of peptides K19 (left) and KK12 (right). The peaks at 1660 $cm^{-1}$ and 1560 $cm^{-1}$ correspond to amide I and amide II bands of the immobilized peptides, respectively.

Peptide linking to the membranes also employed EDC/NHS activation and reaction with the lysine-terminated peptides. However, because IR spectroscopy cannot readily probe the

interior of porous membranes, we used fluorescence spectroscopy to quantify peptide immobilization. Figure 2.3 shows the fluorescence spectra of the peptide standards and calibration curves constructed using the emissions intensities at $\lambda_{max}$ for each peptide. The emissions spectra for both sets of standards (see Figure 2.3) showed a linear increase in emissions intensity with concentration.

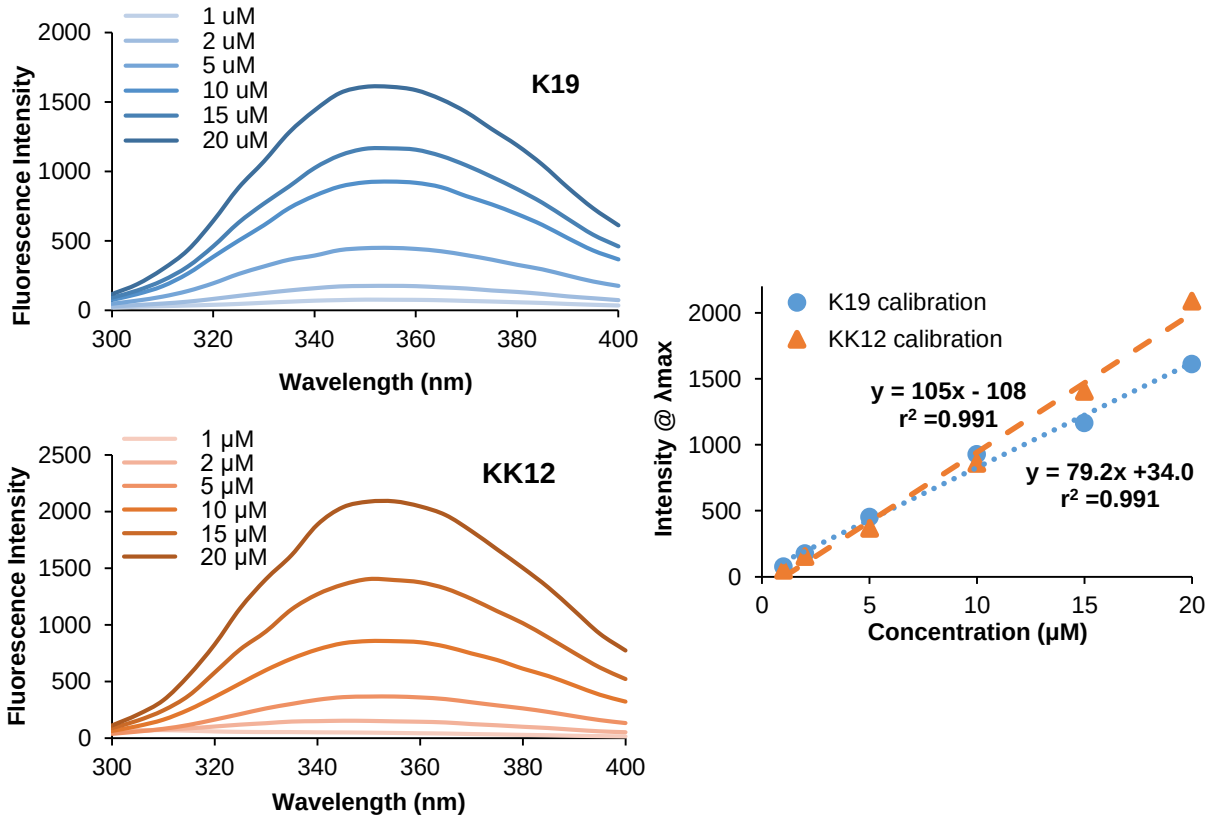


**Figure 2.3.** Fluorescence emission spectra for K19 (blue, top) and KK12 (orange, bottom) standards. Calibration curves based on emission at $\lambda_{max}$ (355 nm for K19 and 350 nm for KK12) in the spectra.

The fluorescence intensity of loading solutions decreased significantly after circulation through the membrane for 2 h (see Figure 2.4), consistent with extensive peptide immobilization. In the case of the KK12, the emissions intensity of the loading solution is almost zero after circulating through the membrane. Based on decreases in fluorescence intensity, membranes captured 27.4 ± 4.0 mg of K19 per mL membrane and 57.6 ± 0.3 mg of KK12 per mL membrane

(see Table 2.1). Particularly for KK12, higher peptide concentrations or larger loading solution volumes may lead to more extensive peptide capture. However, considering the ratio of antibody mass (150 kDa) to peptide mass (1285 Da for KK12 and 2032 Da for K19) and 1:1 binding between peptides and antibodies, antibody binding to either of the peptide-containing membranes would completely fill the membrane several times. Thus, this peptide loading should be sufficient for high-capacity antibody capture.

The average capture of KK12 was double that of K19, ad IR spectra of films on Au-coated wafers show a similar trend. Greater capture of KK12 may occur because the smaller peptide more easily penetrates films activated with EDC/NHS to form covalent bonds. However, KK12 also contains an extra lysine residue, which could lead to more extensive reaction with the activated film.

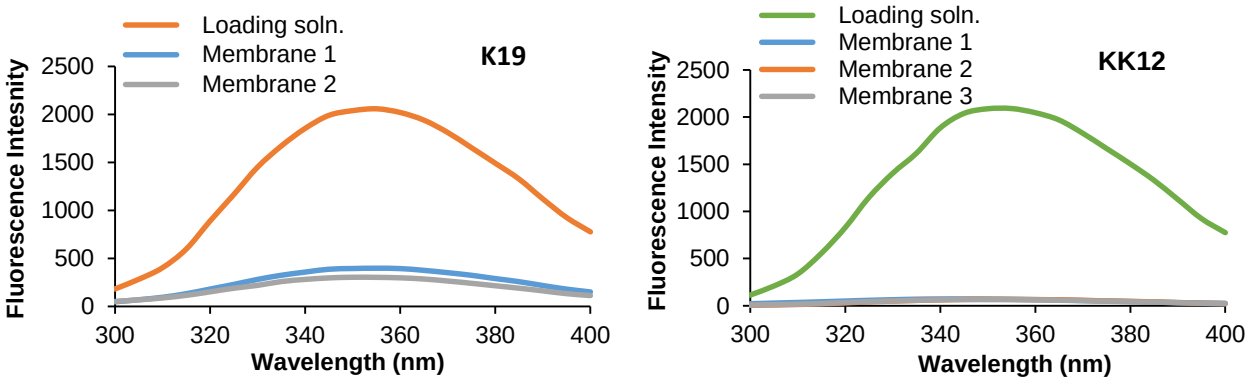


**Figure 2.4.** Fluorescence emission spectra for peptide solutions before (denoted loading) and after circulation (denoted membrane 1, 2, 3) through membranes. The peptide immobilizations shown here used a membrane with a 2.5 cm diameter (0.0346 $cm^3$ vol.).

**Table 2.1.** K19 and KK12 capture in membranes as determined by fluorescence spectroscopy analyses of loading solutions.

| *Peptide* | *Trial* | *Capture (mg/mL)* | *Avg. Capture (mg/mL)* | *± SD* |
|---|---|---|---|---|
| K19 | 1 | 29.2 | 27.4 | 4.0 |
| | 2 | 30.2 | | |
| | 3 | 22.8 | | |
| KK12 | 1 | 57.3 | 57.6 | 0.3 |
| | 2 | 57.8 | | |
| | 3 | 57.8 | | |

### 2.3.2 Antibody capture via Fc-binding peptide KK12

Initially we examined antibody binding to KK12-modified wafers after immersion in 0.1 mg/mL antibody solutions. Because KK12 is a protein A biomimetic peptide, it should capture any IgG antibody. Reflectance FTIR spectra (Figure 2.5) show only a small increase in the amide I band absorbance (1650 $cm^{-1}$) after immersion in the antibody solution. However, elution with 100 mM Gly (pH 2.7) removes the increase in amide absorbance and suggests that the antibody binding real but low. Similar results occurred for both Herceptin and Avastin, consistent with KK12 binding to the Fc-region of these antibodies.

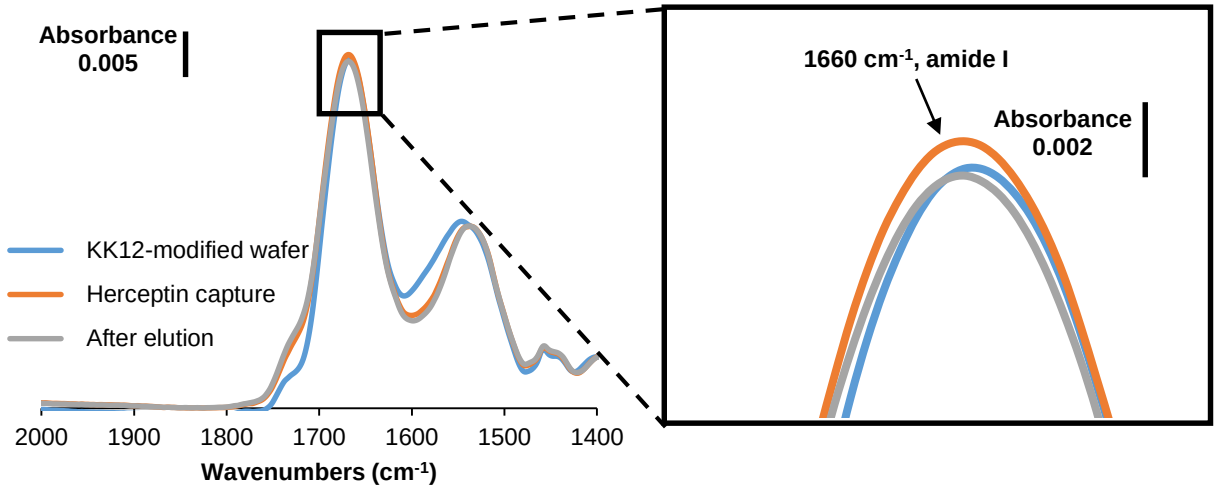


**Figure 2.5.** Reflectance FTIR spectrum of a KK12-modified $(PEI/PAA)_2$ film before (blue) and after immersion in 0.1 mg/mL Herceptin for 1 h and rinsing with water (orange). The figure also shows the film spectrum of the same films after subsequent immersion in 100 mM Gly (pH 2.7) and rinsing with water (gray). The expanded area more clearly shows the changes in amide intensity.

Despite low binding to KK12-modified films on Au-coated wafers, KK12-modified membranes (2.5 cm diameter, 0.0346 $cm^3$ vol.) capture significant amounts of Avastin and Herceptin. Figure 2.6 shows breakthrough curves during passage of either 0.1 mg/mL Avastin or 0.1 mg/mL Herceptin through a membrane modified with PAA/PEI/PAA-KK12 films. Membranes capture nearly all of the antibodies for at least 2 mL of effluent. Based on the differences between the feed and the effluent antibody concentrations for several membranes, the average binding capacities were 9.96 mg/mL for Avastin and 8.40 mg/mL for Herceptin. The similar binding capacities for Herceptin and Avastin are consistent with Fc-binding since both antibodies belong to the IgG isotype.

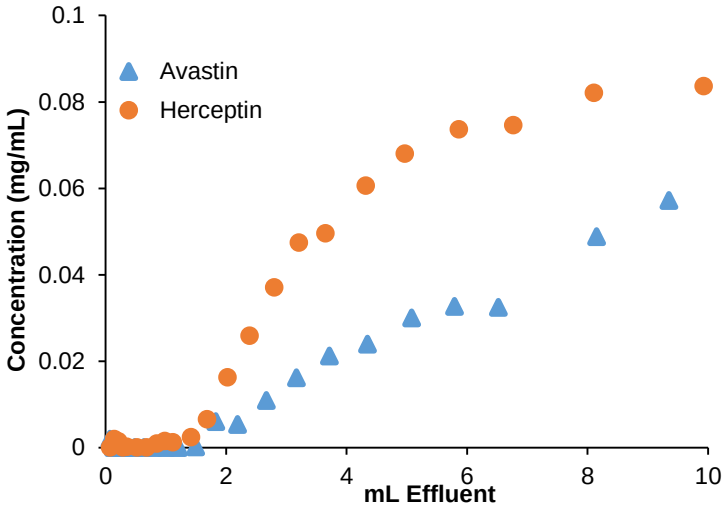


**Figure 2.6.** Breakthrough curves for Avastin and Herceptin capture in KK12-modified membranes. The feed solution contained 0.1 mg/mL antibody. As expected, the membranes captured both antibodies. The binding capacities based on these curves are 8.40 mg/mL for Herceptin (orange) and 9.96 mg/mL for Avastin (blue).

We assessed the reusability of the KK12-modified membranes by eluting antibodies with 100 mM Gly (pH 2.7) and repeating breakthrough curves on the same membrane. After elution, the membranes were regenerated by washing with 10 mL of deionized water and 10 mL 20 mM PBS (no NaCl, pH 7.4). Unfortunately, the Herceptin binding capacity declined to 2.26 mg/mL after the initial binding and elution (see Figure 2.7), suggesting that the membrane is unstable in this harsh elution condition. This may suggest desorption of the polyelectrolyte film from the membrane.

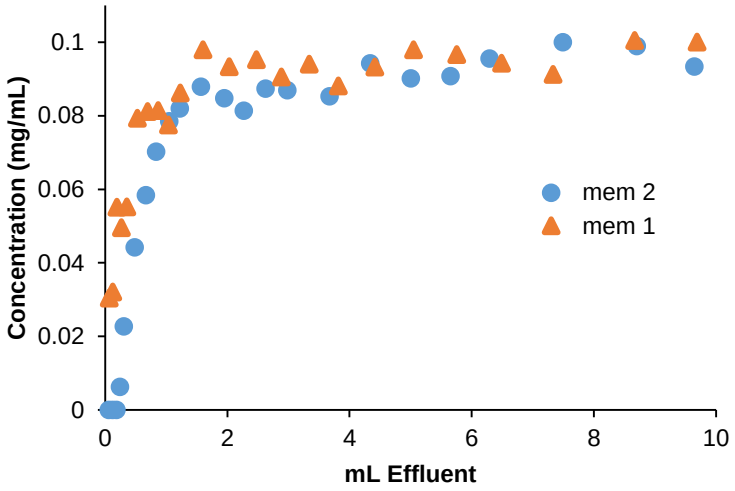


**Figure 2.7.** Second set of Herceptin breakthrough curves for 2 KK12-modified membranes. Initial breakthrough curves for these membranes are similar to the Herceptin plot in Figure 2.6. After initial binding and elution with 100 mM Gly (pH 2.7), the membrane capacity did not return to its initial value. The feed solution contained 0.1 mg/mL antibody.

### 2.3.3 Selective capture of Herceptin via Fab-binding peptide K19

K19 is a HER2-mimetic peptide and, therefore, selectively binds Herceptin. To confirm the selectivity of the K19 mimotope, we immersed K19-modified Au-coated Si wafers in solutions containing either Herceptin or Avastin. After immersion in a 0.1 mg/mL Herceptin solution, reflectance FTIR show a significant increase in the amide I and II bands (Figure 2.8). Moreover, immersion in 2% SDS (100 mM DTT) removes this increase. Similar experiments with Avastin showed no detectable binding. The small decrease in the acid carbonyl peak at 1710 $cm^{-1}$ may stem from deprotonation in the Avastin binding buffer.

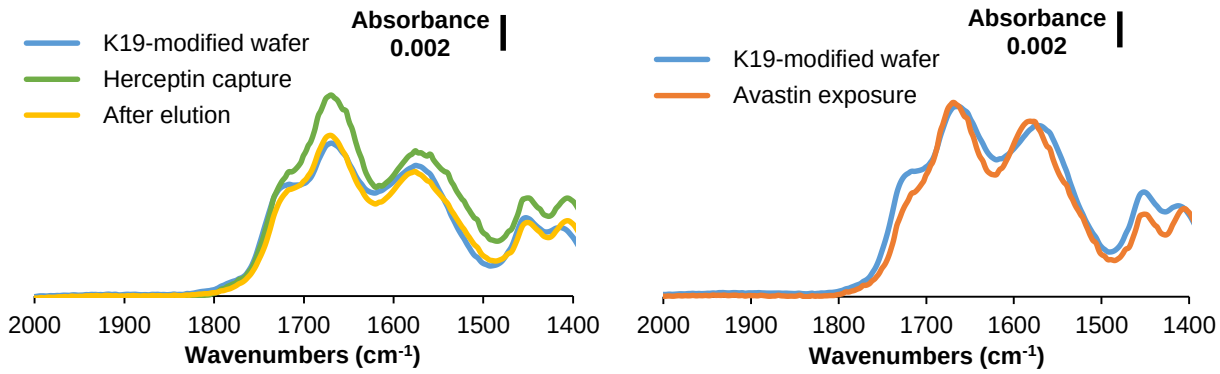


**Figure 2.8.** Reflectance FTIR spectra for K19-modified $(PEI/PAA)_2$ films before (blue) and after immersion in 0.1 mg/mL solutions of Herceptin (left, green) or Avastin (right, orange) for 1 h and rinsing with water. The increase in the amide I and II band intensities suggest successful Herceptin capture, but no discernible increase was seen after immersion in the Avastin solution. The spectrum after immersion in 2% SDS (100 mM DTT) for 30 minutes and rinsing with water (left, yellow) removed the increase seen after immersion in the Herceptin solution.

We calculated the Herceptin and Avastin binding capacities of K19-modified membranes using breakthrough curves determined with Bradford assays. Figure 2.9 shows breakthrough curves for both large (2.5 cm diameter, 0.0346 $cm^3$ vol.) and small (1.0 cm diameter, 0.00864 $cm^3$ vol.) membranes. The Herceptin binding capacity (based on the average of both large and small membranes) was 16.3 ± 1.14 mg/mL. In contrast, the Avastin binding capacity was 2.6 mg/mL. The small amount of calculated Avastin binding may stem from dead volume in the system or a minimal amount of non-specific binding. The membrane selectivity is consistent with the FTIR spectra in Figure 2.8. Not only did the K19-modified membranes selectively bind Herceptin, but they also exhibited a higher binding capacity than KK12-modified membranes despite having 50% lower peptide immobilization (section 2.3.1). Since the K19 HER2-mimotope binds Herceptin at the Fab region, the K19-Herceptin interaction is characteristic of the strong interaction between an antibody and its antigen. The increased binding capacity may stem from the strength and specificity of this interaction, although it is possible that a lower density of immobilized peptide leads to more antibody binding due to less steric hindrance.

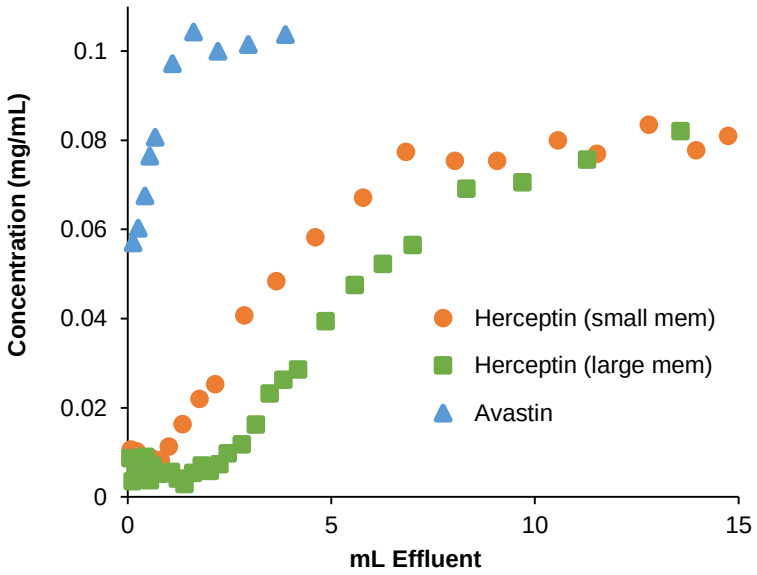


**Figure 2.9.** Breakthrough curves for Avastin and Herceptin on K19-modified membranes. The feed solution contained 0.1 mg/mL antibody. The Herceptin binding capacity was 16.3 ± 1.14 mg/mL, whereas the Avastin binding capacity was 2.6 mg/mL. The selectivity of the membrane is consistent with a Fab-binding peptide.

### 2.3.4 Purification of Herceptin from human serum

To further demonstrate the selectivity of the K19-modified membranes, we spiked Herceptin into diluted human serum – a protein cocktail of mostly albumin and various IgG isotype antibodies. We passed the Herceptin-spiked serum through a K19-modified membrane and eluted the bound antibody with 2% SDS (100 mM DTT). In the SDS-PAGE gel, two bands appear in the lane of the SDS eluate (Figure 2.10, lane 4). These bands at 25 kDa and 50 kDa correspond to the antibody light and heavy chains, respectively. We also passed human serum with no Herceptin through a K19-modified membrane, and the eluate exhibited no bands in the SDS-PAGE gel (Figure 2.10, lane 6). Therefore, K19-modified membranes exhibit low non-specific binding and discriminate between antibodies of the same isotype to selectively bind Herceptin.

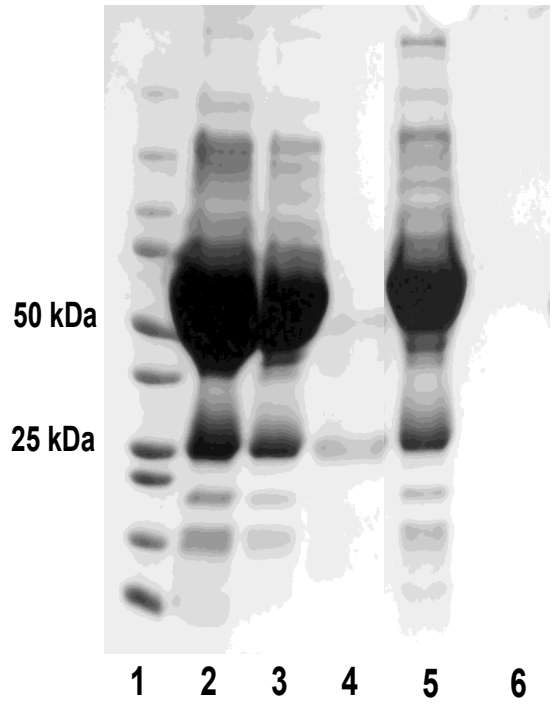


**Figure 2.10.** SDS-PAGE analysis of Herceptin purification from human serum. Diluted serum with or without 0.1 mg/mL Herceptin was passed through a K19-modified membrane, and bound antibody was eluted with 2% SDS. Lanes *(1)* Molecular weight ladder, *(2)* Herceptin-spiked solution, *(3)* Spiked serum after passing through the membrane, *(4)* 2% SDS eluate from the membrane loaded with spiked serum, *(5)* Unspiked serum after passing through the membrane, *(6)* 2% SDS eluate from the membrane loaded with unspiked serum.

#### 2.3.4.1 Challenges with elution of high-affinity antibodies

Elution of Herceptin from the K19-modified membranes required detergent solutions, as traditional elution methods such as 3 M KSCN and 100 mM Gly (pH 2.7) were ineffective according to initial SDS-PAGE analyses and reflectance FTIR analyses on Au-coated Si wafers. Not even pH 2.0 conditions were harsh enough to break the Herceptin-K19 interaction, and below this pH the $(PEI/PAA)_2$ films are likely unstable. While the strength and specificity of the Herceptin-epitope interaction give rise to an effective therapeutic, they also make Herceptin elution from the membrane difficult. Moreover, detergent elutions are not compatible with downstream analyses such as mass spectrometry and Bradford assays. Although detergent-removal methods exist,[22,23] they introduce sample loss and extra costs into the purification

process. A more effective elution mechanism may enable Herceptin analysis directly after isolation with a membrane. Section 4.2.1 describes preliminary work on an acid-labile linker that could serve in universal elution method for high-affinity interactions such as the Herceptin-K19 binding.

## 2.4 Conclusions

Amide coupling of lysine residues to PAA effectively immobilizes peptides onto polyelectrolyte films. Nylon membranes containing PAA/PEI/PAA films can immobilize at least 57.6 ± 0.3 mg of KK12 per mL of membrane and 27.4 ± 4.0 mg of K19 peptide per mL of membrane. The greater immobilization of KK12 relative to K19 may stem from either the smaller size of KK12 or its extra out-of-plane lysine residue.

However, the extent of peptide immobilization does not correlate with the amount of antibody that binds to these peptides in a membrane. Despite its high peptide content, the KK12-modified membrane captured only 9.96 mg/mL of Avastin and 8.40 mg/mL of Herceptin. In contrast, the K19-modified membrane captured 16.3 ± 1.14 mg/mL of Herceptin. Although the antibodies easily eluted (100 mM Gly, pH 2.7) from KK12-modified membranes, the binding capacity dropped 75% after the initial binding and elution. Rapid capture of IgG antibodies can occur using a membrane-bound Fc-binding peptide, but membrane reuse is ineffective. Further studies with other Fc-binding peptides and membranes are needed to obtain a potential alternative to protein A columns.

The KK12-modified membranes exhibit no selectivity between Avastin and Herceptin, because KK12 binds to the Fc region of IgG antibodies. The K19-modified membranes,

however, selectively capture Herceptin since the K19 peptide mimics the HER2 antigen binding site. The binding capacity for Avastin on K19-modified membranes was at most 2.6 mg/mL – and part of this capture may stem from dead volume in the system – whereas the binding capacity for Herceptin was 16.3 ± 1.14 mg/mL. Additionally, K19-modified membranes successfully selectively captured Herceptin from human serum with minimal non-specific binding. Membranes that selectively capture a specific antibody may prove effective in techniques for determining the levels of therapeutic antibodies in complex matrices such as human plasma. Such techniques would help to determine when a new dose of very expensive antibody is necessary.

Herceptin elution from the K19-modified membranes, however, is challenging. The Herceptin-K19 bond is hard to break under conditions that are amenable to downstream analyses. Thus, Herceptin detection methods will require a more effective elution method that does not depend on the strength of the antibody-antigen interaction. Section 4.3.1 discusses preliminary work with an acid-labile linker for peptide immobilization.

# REFERENCES

REFERENCES


(1) Cho, H.-S.; Mason, K.; Ramyar, K. X.; Stanley, A. M.; Gabelli, S. B.; Denney, D. W.; Leahy, D. J. Structure of the Extracellular Region of HER2 Alone and in Complex with the Herceptin Fab. *Nature* **2003**, *421*, 756–760.

(2) Kim, K. J.; Li, B.; Houck, K.; Winer, J.; Ferrara, N. The Vascular Endothelial Growth Factor Proteins: Identification of Biologically Relevant Regions by Neutralizing Monoclonal Antibodies. *Growth Factors* **1992**, *7* (1), 53–64.

(3) Presta, L. G.; Chen, H.; O'Connor, S. J.; Chisholm, V.; Meng, Y. G.; Krummen, L.; Winkler, M.; Ferrara, N. Humanization of an Anti-Vascular Endothelial Growth Factor Monoclonal Antibody for the Therapy of Solid Tumors and Other Disorders. *Cancer Res.* **1997**, *57* (20), 4593–4599.

(4) Chames, P.; Van Regenmortel, M.; Weiss, E.; Baty, D. Therapeutic Antibodies: Successes, Limitations and Hopes for the Future. *Br. J. Pharmacol.* **2009**, *157* (2), 220–233.

(5) Aldington, S.; Bonnerjea, J. Scale-up of Monoclonal Antibody Purification Processes. *J. Chromatogr. B* **2007**, *848* (1), 64–78.

(6) Sadana, B. A. M. Efficiency and Economics of Bioseparation: Some Case Studies. *Bioseparation* **1994**, *4* (4), 221–235.

(7) Low, D.; O'Leary, R.; Pujar, N. S. Future of Antibody Purification. *J. Chromatogr. B* **2007**, *848* (1), 48–63.

(8) Tsai, C. W.; Jheng, S. L.; Chen, W. Y.; Ruaan, R. C. Strategy of Fc-Recognizable Peptide Ligand Design for Oriented Immobilization of Antibody. *Anal. Chem.* **2014**, *86* (6), 2931–2938.

(9) Jeong, Y. jin; Kang, H. J.; Bae, K. H.; Kim, M. G.; Chung, S. J. Efficient Selection of IgG Fc Domain-Binding Peptides Fused to Fluorescent Protein Using E. Coli Expression System and Dot-Blotting Assay. *Peptides* **2010**, *31* (2), 202–206.

(10) Sugita, T.; Katayama, M.; Okochi, M.; Kato, R.; Ichihara, T.; Honda, H. Screening of Peptide Ligands That Bind to the Fc Region of IgG Using Peptide Array and Its Application to Affinity Purification of Antibody. *Biochem. Eng. J.* **2013**, *79*, 33–40.

(11) Yang, H.; Gurgel, P. V.; Carbonell, R. G. Purification of Human Immunoglobulin G via Fc-Specific Small Peptide Ligand Affinity Chromatography. *J. Chromatogr. A* **2009**, *1216* (6), 910–918.

(12) Zhao, W. W.; Shi, Q. H.; Sun, Y. FYWHCLDE-Based Affinity Chromatography of IgG: Effect of Ligand Density and Purifications of Human IgG and Monoclonal Antibody. *J. Chromatogr. A* **2014**, *1355*, 107–114.

(13) Wei, Y.; Xu, J.; Zhang, L.; Fu, Y.; Xu, X. Development of Novel Small Peptide Ligands for Antibody Purification. *RSC Adv.* **2015**, *5* (82), 67093–67101.

(14) Lund, L. N.; Gustavsson, P. E.; Michael, R.; Lindgren, J.; Nørskov-Lauritsen, L.; Lund, M.; Houen, G.; Staby, A.; St. Hilaire, P. M. Novel Peptide Ligand with High Binding Capacity for Antibody Purification. *J. Chromatogr. A* **2012**, *1225*, 158–167.

(15) Jiang, B.; Liu, W.; Qu, H.; Meng, L.; Song, S.; Ouyang, T.; Shou, C. A Novel Peptide Isolated from a Phage Display Peptide Library with Trastuzumab Can Mimic Antigen Epitope of HER-2. *J. Biol. Chem.* **2005**, *280* (6), 4656–4662.

(16) Shang, Y.; Singh, P. R.; Chisti, M. M.; Mernaugh, R.; Zeng, X. Immobilization of a Human Epidermal Growth Factor Receptor 2 Mimotope-Derived Synthetic Peptide on Au and Its Potential Application for Detection of Herceptin in Human Serum by Quartz Crystal Microbalance. *Anal. Chem.* **2011**, *83*, 8928–8936.

(17) Leo, N.; Shang, Y.; Yu, J.; Zeng, X. Characterization of Self-Assembled Monolayers of Peptide Mimotopes of CD20 Antigen and Their Binding with Rituximab. *Langmuir* **2015**, *31* (51), 13764–13772.

(18) Datta, S.; Cecil, C.; Bhattacharyya, D. Functionalized Membranes by Layer-By-Layer Assembly of Polyelectrolytes and In Situ Polymerization of Acrylic Acid for Applications in Enzymatic Catalysis. *Ind. Eng. Chem. Res.* **2008**, *47* (14), 4586–4597.

(19) Bhattacharjee, S.; Dong, J.; Ma, Y.; Hovde, S.; Geiger, J. H.; Baker, G. L.; Bruening, M. L. Formation of High-Capacity Protein-Adsorbing Membranes through Simple Adsorption of Poly(acrylic Acid)-Containing Films at Low pH. *Langmuir* **2012**, *28* (17), 6885–6892.

(20) Sousa, M. M.; Steen, K. W.; Hagen, L.; Slupphaug, G. Antibody Cross-Linking and Target Elution Protocols Used for Immunoprecipitation Significantly Modulate Signal-to Noise Ratio in Downstream 2D-PAGE Analysis. *Proteome Sci.* **2011**, *9* (1), 45.

(21) Conley, R. T. Interpretation of Infrared Spectra, Part II: Common Functional Groups. In *Infrared Spectroscopy*; Allyn and Bacon, Inc.: Boston, MA, 1966; pp 110–175.

(22) Fox, J. L.; Stevens, S. E.; Taylor, C. P.; Poulsen, L. L. SDS Removal from Protein by Polystyrene Beads. *Anal. Biochem.* **1978**, *87* (1), 253–256.

(23) Puchades, M.; Westman, A.; Blennow, K.; Davidsson, P. Removal of Sodium Dodecyl Sulfate from Protein Samples prior to Matrix-Assisted Laser Desorption/ionization Mass Spectrometry. *Rapid Commun. Mass Spectrom.* **1999**, *13* (5), 344–349.

*The C-peptide capture work was done in conjunction with Cody Pinger of the Spence Research Group. He performed ELISA quantification of C-peptide.*

# Chapter 3. Membrane-bound antibodies for protein purification

## 3.1 Introduction

Immunoprecipitation is the most common affinity chromatography method for protein purification.[1] This technique typically employs agarose bead columns, but slow diffusion into bead pores leads to long capture times, and columns often suffer from high pressure drops.[2] Due to their small thicknesses and convective transport in their pores, antibody-containing membranes should enable rapid antigen capture and fast washing and elution with low pressure drops. With recent advances in membrane binding capacities through pore modification via LBL adsorption of polyelectrolyte multilayers or growth of polymer brushes,[3-6] membranes can facilitate rapid and effective high-throughput protein purification. Although immunoprecipitation is widespread, development of high-specificity antibodies that bind the target protein is often expensive or time-consuming. The advent of affinity tags, however, allows researchers to select from a few common anti-tag antibodies for protein purification.[7,8] Common affinity tags include FLAG, polyhistidine, heavy chain protein C (HPC) and hemagglutinin A.[7,9,10] Affinity tags fall into two main classes: those that bind to immobilized small-molecule ligands and those that bind to immobilized protein.[9] Recent research exploited the advantages of membranes to isolate proteins with the first class of affinity tags. Specifically, immobilized metal-ion complexes captured polyhistidine-tagged proteins from cell lysate.[11-16] This research focuses on applying the

advantages of membranes to purify proteins with affinity tags that bind to immobilized anti-tag antibodies.

Antibody immobilization in membranes can occur through electrostatic or covalent anchoring or a two-step immobilization that combines the two types of bonding (see Figure 1.6).[17-19] The two-step immobilization offers the high capacity of electrostatic immobilization while preserving the stability of direct covalent immobilization. The research described in this thesis uses the two step protocol to immobilize anti-hemagglutinin A (anti-HA) antibodies in PEM-modified nylon membranes. Subsequently, these membranes capture HA-tagged regulator G signaling protein 2 (RGS2). RGS2 plays key roles in several important cardiovascular disorders, such as myocardial hypertrophy[20], atrial arrhythmias[21] and hypertension[22] and also suppresses breast cancer cell growth.[23] This research aims to purify HA-RGS2 from cell lysate to enable downstream analysis via MS and identify post-translational modifications such as phosphorylation.

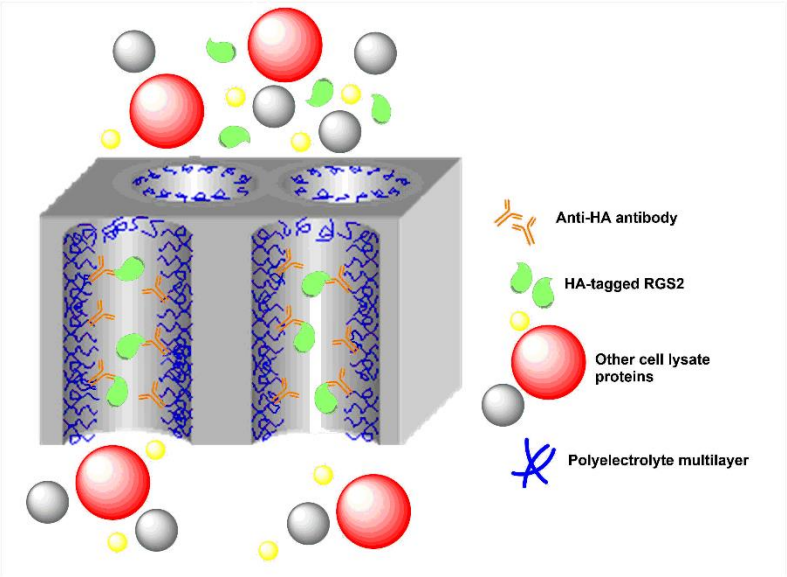


**Figure 3.1.** Illustration of membrane-based selective capture of HA-tagged RGS2 from cell lysate. Capture employs immobilized antibodies.

In addition to capturing tagged proteins, immobilized antibodies can also bind native proteins and peptides. I immobilized anti-(C-peptide) antibodies in PEM-modified polycarbonate (PC) membranes for C-peptide capture. The pancreas co-secretes C-peptide with insulin, and this peptide plays a key role in insulin synthesis as well as ATP release from and glucose uptake in red blood cells.[24-26] This research aims to use small anti-(C-peptide) membranes in a microfluidic device to capture C-peptide from cell secretions as the secretions diffuse across the membrane and into the microfluidic channel. Studying changes in ATP release and glucose clearance in the presence and absence of C-peptide in cell secretions may lead to a more complete understanding of the role C-peptide plays in these crucial biological processes and cell-to-cell communications.

## 3.2 Experimental

### 3.2.1 Materials

Sheets of hydroxylated nylon membranes (LoProdyne® LP, pore size=1.2 μm, thickness=110 μm, 50% porosity) were obtained from Pall Corporation and cut into 25 mm disks. Polycarbonate membranes (Whatman® Cyclopore®, track-etched, pore size=0.4 or 1.0 μm, thickness=10 μm, 4-20% porosity) were purchased from Sigma-Aldrich and cut into 25 mm disks. Au-coated silicon wafers (200 nm sputtered Au on 20 nm Cr on Si) were obtained from Addison. Poly(acrylic acid) (PAA, $M_w$=100,000 Da, 35% in water) was purchased from Sigma-Aldrich and branched polyethyleneimine (PEI, $M_w$=250,000 Da) was purchased from Aldrich. Aqueous solutions of 0.01 M PAA (repeat unit concentration in 0.5 M NaCl, pH 3) and 2.0 mg/mL PEI (pH 3) were prepared in deionized water (18.2 MΩcm, Milli-Q), and the pH values of the solutions were adjusted by adding 0.1 M HCl or 0.1 M NaOH dropwise. 1-Ethyl-3-(3-

dimethylaminopropyl)carbodiimide hydrochloride (EDC) and N-hydroxysuccinimide (NHS) were purchased from Sigma-Aldrich. Anti-hemagglutinin antibody (Y-11, rabbit polyclonal, 200 μg/mL stock) was purchased from Santa Cruz Biotechnology. Hemagglutinin-transfected RGS2-containing cell lysate was provided by Dr. Benita Sjogren of, Michigan State University, Department of Pharmacology and Toxicology. Anti-(C-peptide) antibody (1H8, mouse monoclonal, 2.0 mg/mL stock) was purchased from Abcam. Mouse C-peptide solutions and mouse C-peptide, $Zn^{2+}$ and mouse insulin solutions were provided by Dr. Dana Spence of Michigan State University, Department of Chemistry. Mouse C-peptide ELISA kits were acquired from Eagle Biosciences.

### 3.2.2 Immobilization of antibodies

Antibodies were immobilized via the two-step immobilization method developed by Qu, *et. al*.[59] and shown in Figure 1.6. For anti-HA immobilization, nylon membranes (2.5 cm diameter, 0.0364 $cm^3$ vol.) were first cleaned and modified with a PAA/PEI/PAA film as outlined in section 2.2.2. After washing with deionized water for 10 minutes, 0.1 mg/mL antibody in 20 mM PBS (no NaCl, pH 4.5) was circulated through the membrane at a flow rate of 1.0 mL/min for 2 hours to electrostatically immobilize the antibody. Without washing the membrane with water, 10 mL of aqueous 5 mM EDC solution (pH 4.5) was circulated through the membrane for 1 hour to covalently link the antibody to the membrane. The membrane was subsequently washed with deionized water for 10 minutes. Using Nanodrop UV/Vis (Thermo Fisher NanoDrop 2000) spectroscopy, the antibody feed solution was analyzed before and after passing through the membrane to quantify antibody immobilization. For anti-(C-peptide) immobilization, we tested 1.0 μm and 0.4 μm pore polycarbonate (PC) membranes. PAA/PEI/PAA films were adsorbed on

the 1.0 μm pore PC membranes, and a single layer of PAA was adsorbed on the 0.4 μm pore PC membranes as in section 2.2.2. The PAA-modified membranes were cut into smaller membranes (1.0 cm diameter, 0.000785 $cm^3$ vol.), and anti-(C-peptide) was immobilized and quantified in the same manner as anti-HA. The quantification of antibody immobilization was calculated using 0.02, 0.04, 0.06, 0.08 and 0.10 mg/mL Avastin antibody standards.

### 3.2.3 HA-tagged RGS2 purification from cell lysate

The polyelectrolyte film-modified membranes were cut into smaller membranes (1.0 cm diameter, 0.00864 $cm^3$ vol.). Anti-HA antibody was immobilized as in section 3.2.2 and monitored via Nanodrop UV/Vis spectroscopy. After immobilization, 10 mL of 20 mM PBS (137 mM NaCl, pH 7.4) was passed through the membrane. Cell lysate (250 μL) containing HA-tagged RGS2 protein (HA lysate) was diluted 1:4 and circulated through the membrane for 30 minutes at a flow rate of 1.0 mL/min. The protein content for the cell lysate ranged from 8-11 mg total protein and 1 μg RGS2. Aliquots of feed effluent solutions were collected for western blot and SDS-PAGE analyses. Several buffers were employed to remove non-specifically bound protein, including 1 mL aliquots of 20 mM PBS (137 mM NaCl, pH 7.4) and 20 mm PBS (500 mM NaCl, pH 7.4) and, in subsequent experiments, 100 mM acetic acid/acetate buffer (pH 4.7). Several elution protocols were employed as well – 5% formic acid (pH 2.0), 100 mM Gly (pH 2.7) and 100 mM DTT were passed through the membrane in succession to determine their effectiveness. Each buffer wash and elution were analyzed via western blot and SDS-PAGE gel electrophoresis.

Control experiments were performed in the same manner with non-transfected lysate (NT lysate) on (anti-HA)-modified, PAA-modified and bare nylon membranes to monitor non-specific binding. The feed lysate, effluent lysate, buffer washes and elution were analyzed via western blot and SDS-PAGE.

### 3.2.4 C-peptide capture

The affinity of C-peptide to the anti-(C-peptide) was first monitored by passing a 25 nM C-peptide solution in 20 mM PBS (137 mM NaCl, pH 7.4) through the membrane at 0.5 mL/min. The feed and effluent solutions were analyzed via C-peptide ELISA to quantify C-peptide binding. Control experiments were conducted in the same manner on bare polycarbonate membranes and PAA-modified membranes without antibodies.

## 3.3 Results and discussion

### 3.3.1 Quantification of antibody immobilization

The first step in this work is quantitation of antibody immobilization. Thus, I analyzed the feed and effluent solutions employed to immobilize both anti-HA and anti-(C-peptide)

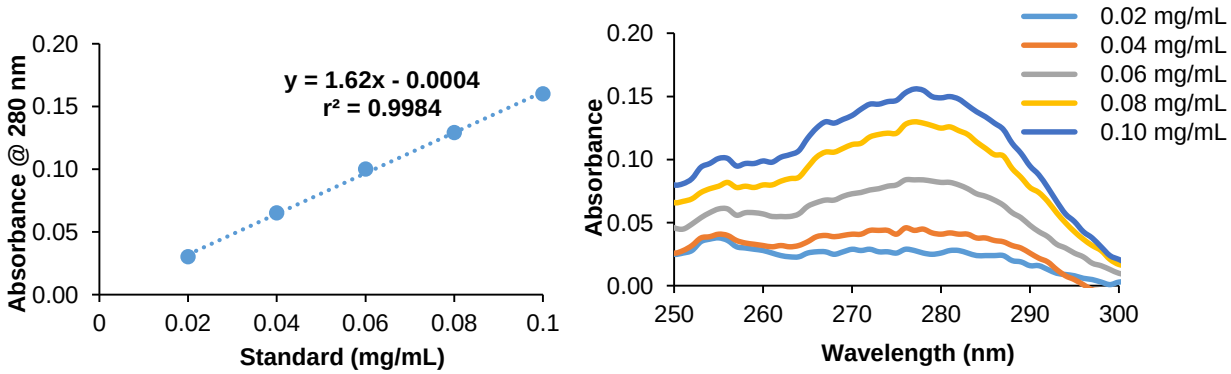


**Figure 3.2.** Nanodrop UV/Vis calibration curve (left) and standard spectra (right) for Avastin standards.

antibodies. Avastin was diluted from a 1.0 mg/mL stock solution to 0.02, 0.04, 0.06, 0.08 and 0.10 mg/mL standards with 20 mM PBS (no NaCl, pH 4.5) and Nanodrop UV/Vis spectroscopy yielded a linear calibration (see Figure 3.2). Spectra of feed and effluent solutions suggest immobilization of both antibodies. However, the anti-HA feed solution exhibited a higher absorbance than the 0.10 mg/mL Avastin standard. The higher absorbance may stem from 0.1% sodium azide and 0.1% gelatin in the stock anti-HA solution. It is also possible that the few variable amino acids in the antibody can alter its absorbance relative to Avastin. Nevertheless, the anti-HA absorbance dropped 75% from the feed solutions to the effluent solutions (see Figure 3.3a). Anti-(C-peptide) effluent solutions showed a similar drop in absorbance (Figure 3.3b), and capacities in 1.0 μm and 0.4 μm pore PC membranes (1.0 cm diameter, 0.000785 $cm^3$ vol.) were 40.6 mg/mL and 53.1 mg/mL, respectively. Assuming a 1:1 binding relationship with the antibodies and their respective antigens, enough antibody is present in the membrane to bind all HA-RGS2 in 1 mL of diluted feed solution, which contains at least 250 ng RGS2, and all C-peptide in 200 μL of feed solution, which contains 5 pmoles of C-peptide.

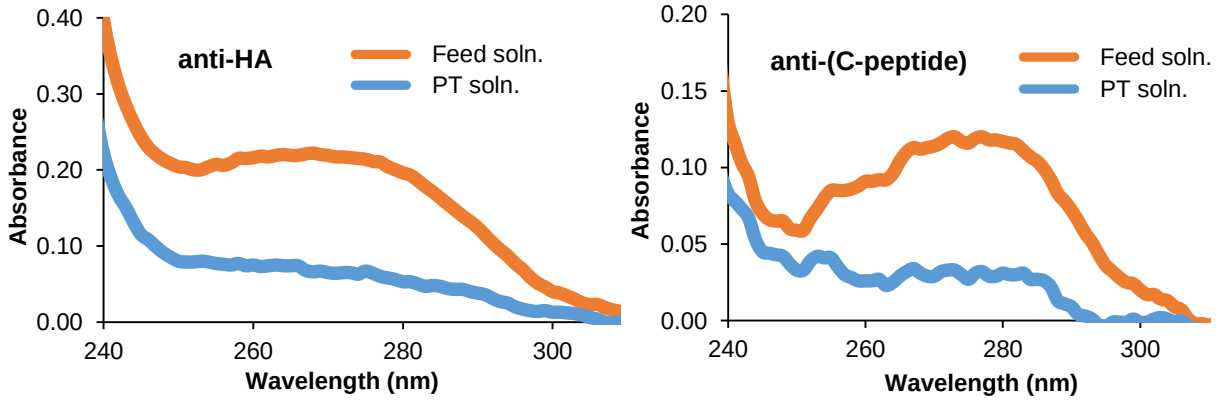


**Figure 3.3.** Nanodrop UV/Vis spectra for anti-HA (left) and anti-(C-peptide) (right) antibody feed and effluent solutions before (orange) and after (blue) circulation through a membrane.

### 3.3.2 HA-RGS2 purification from cell lysate via immobilized anti-HA antibody

For antigen isolation, we first attempted to capture HA-RGS2 proteins from a transfected lysate (HA lysate). I immobilized anti-HA antibody via a two-step linking mechanism (see Figure 1.6.), passed diluted HA lysate containing HA-RGS2 through the membrane and examined several protocols for rinsing and elution of HA-RGS2. Rinsing included two 20 mM PBS (137 mM NaCl, pH 7.4) buffer washes to remove non-specifically bound protein from the membrane before elution with 100 mM Gly (pH 2.7), 5% formic acid (pH 2.0), 0.5% SDS and 2.0% SDS in succession. The Western blot in Figure 3.4 shows that 100 mM Gly and 5% formic acid elute most of HA-RGS2 from the membrane. The 5% formic acid elution seemed more effective than the 100 mM Gly and left very little HA-RGS2 bound to the membrane. However, the SDS-PAGE shows significant amounts of other proteins eluting from the membrane.

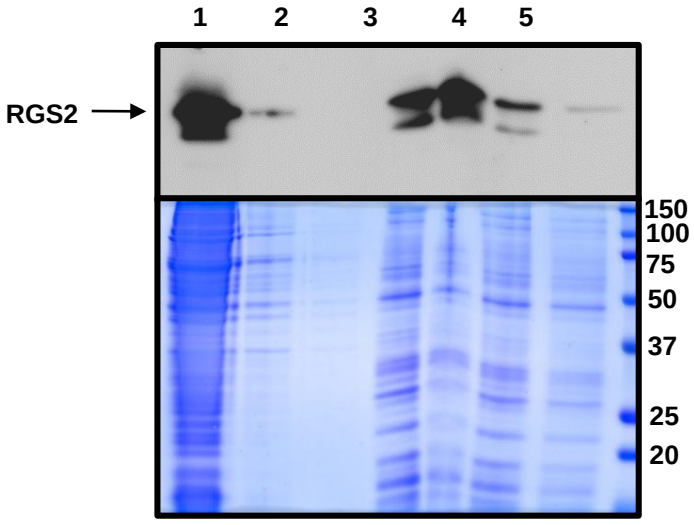


**Figure 3.4.** Western blot (top) and SDS-PAGE analyses (bottom) of effluents and eluates from membrane-based isolation of HA-RGS2. Lanes 1-3 correspond to the effluent lysate, 137 mM NaCl wash 1 and 137 mM NaCl wash 2, respectively. Lanes 4-7 correspond to the 100 mM Gly, 5% formic acid, 0.5% SDS and 2% SDS elution tests, respectively.

Because elution with 5% formic acid is desirable for downstream protein digestion and MS analysis and Figure 3.4 suggests this solution effectively elutes HA-RGS2, we next used 5%

formic acid to elute the protein followed sequentially by 100 mM Gly and 100 mM DTT. To reduce non-specific binding, we rinsed the membrane with two 1 mL aliquots of 20 mM PBS (137 mM NaCl, pH 7.4) and 1 mL of 20 mM PBS (500 mM NaCl, pH 7.4) prior to the elution. Figure 3.5 (Western blot, top) shows that 5% formic acid removed nearly all of the HA-RGS2 from the membrane (lane 12), 100 mM Gly did not remove any HA-RSG2 (lane 13) and 100 mM DTT removed, presumably, any remaining HA-RGS2 (lane 14). Again, however, SDS-PAGE showed significant amounts of non-specifically bound proteins in the 5% formic acid and 100 mM DTT eluents (lane 12).

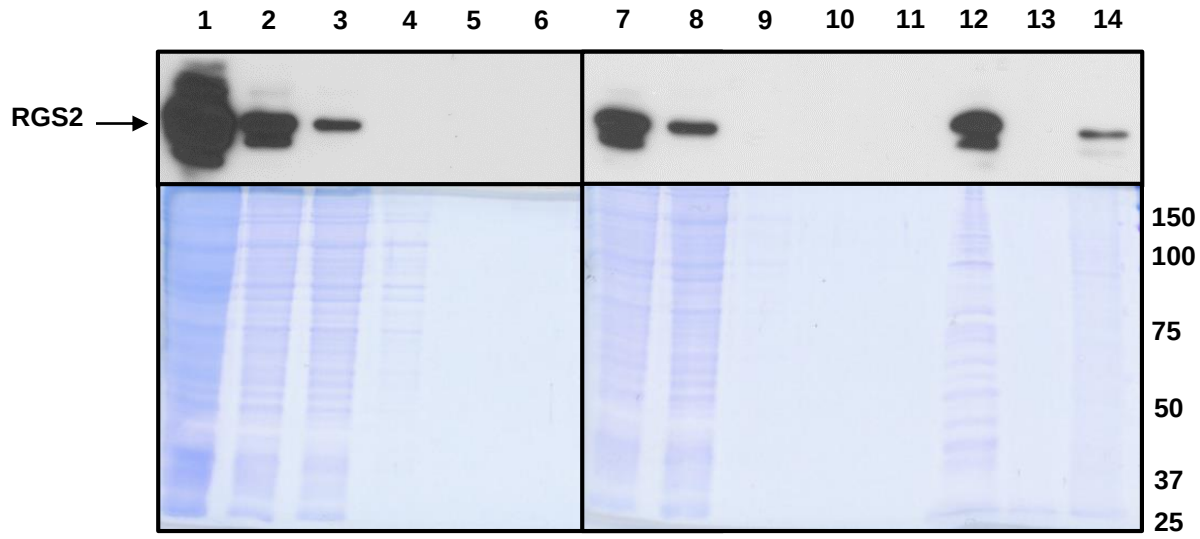


**Figure 3.5.** Western blot (top) and SDS-PAGE analyses (bottom) of effluents from membrane-based isolation of HA-RGS2. HA lysate was passed through two different membranes. The membranes were then stacked for the elution tests. Lane 1 corresponds to the original, undiluted lysate. Lanes 2-6 correspond to the effluent lysate (diluted 1:3 before circulation), 137 mM NaCl wash 1, 137 mM NaCl wash 2 and 500 mM NaCl wash for membrane 1, respectively. Lanes 7-11 correspond to the feed lysate, 137 mM NaCl wash 1, 137 mM NaCl wash 2 and 500 mM NaCl wash for membrane 2, respectively. Lanes 12-14 correspond to the 5% formic acid, 100 mM Glycine and 100 mM DTT elution tests, respectively.

To further reduce non-specific binding, I passed 100 mM acetate buffer (pH 4.7) through the membrane following two 1 mL 20 mM PBS (137 mM NaCl, pH 7.4) washes and one 1 mL 20 mM PBS (500 mM NaCl, pH 7.4) wash. Figure 3.6 (Western blot, lane 3) shows that acetate buffer did not remove any detectable amount of HA-RGS2 from the membrane, but it did

remove some non-specifically bound proteins (SDS-PAGE, lane 3), most notably higher molecular weight proteins. Significant amounts of other proteins were still present, however, in the 5% formic acid elution (SDS-PAGE, lane 2), suggesting that the acetate buffer did not remove all non-specifically-bound proteins.

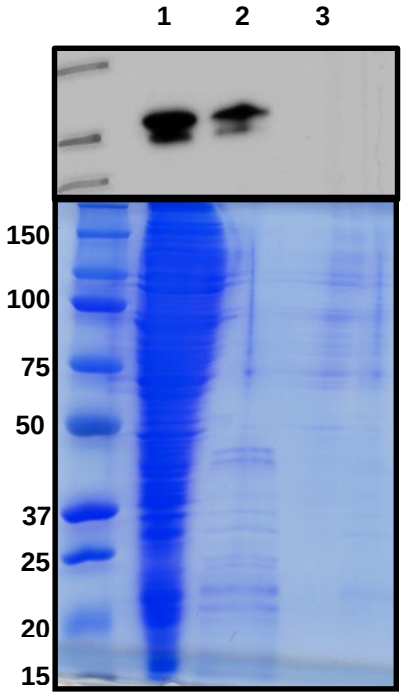


**Figure 3.6.** Western blot (top) and SDS-PAGE (bottom) analyses of effluents and eluates from membrane-based isolation of RGS2 with a 100 mM acetate buffer (pH 4.7) wash. Lanes 1-3 correspond to the effluent lysate, 5% formic acid elution and 100 mM acetate buffer wash, respectively. Acetate buffer removed some of the higher molecular weight protein, but the 5% formic acid elution showed non-specifically bound proteins.

To determine the reason for the non-specific adsorption, I performed control experiments with non-transfected lysate (NT lysate) passing through bare nylon membranes, PAA-modified membranes and anti-HA membranes. After loading the membrane with 1 mL diluted lysate (250 µL diluted 1:3), I passed 1 mL of 20 mM PBS (137 mM NaCl, pH 7.4), 1 mL of 20 mM PBS (500 mM NaCl, pH 7.4) and 1 mL of 100 mM acetate buffer (pH 4.7) sequentially through each membrane. The SDS-PAGE in Figure 3.6 suggests that both nylon and PAA-modified

membranes experience a significant degree of non-specific adsorption that is hard to remove in buffers, but the anti-HA membrane showed almost no non-specific adsorption. The low non-specific adsorption on the antibody-containing membranes is difficult to reconcile with the non-specific adsorption when using HA lysate (see Figures 3.5 and 3.6). Perhaps binding of HA-RGS2 creates a surface that is much more prone to non-specific adsorption.

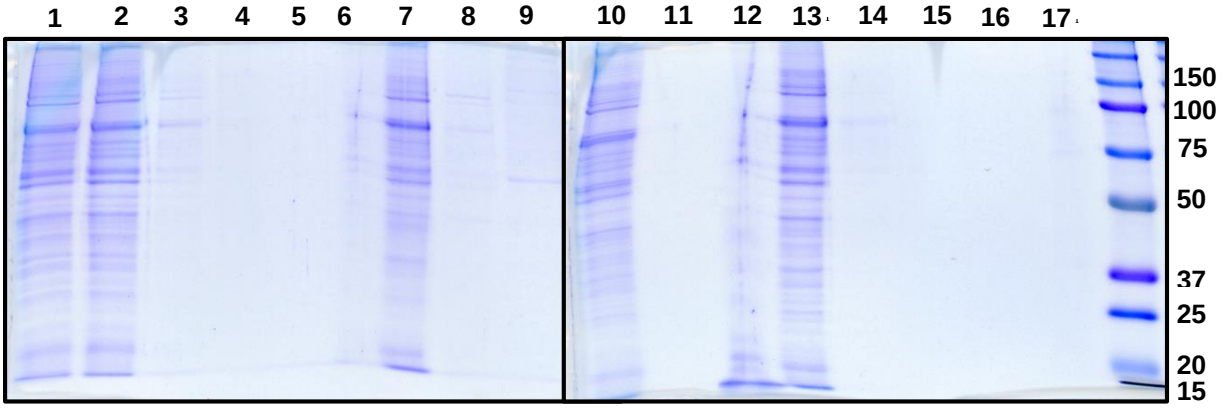


**Figure 3.7.** SDS-PAGE analyses of non-specific binding during passage of NT lysate through bare, PAA-modified and anti-HA containing nylon membranes. Lanes 1-6 correspond to the feed lysate, effluent lysate, 137 mM NaCl wash, 500 mM NaCl wash, 100 mM acetate buffer wash and 5% formic acid elution, respectively, on a bare nylon membrane. Lanes 7-12 correspond to the effluent lysate, 137 mM NaCl wash, 500 mM NaCl wash, 100 mM acetate buffer wash and 5% formic acid elution, respectively, on a PAA-modified membrane. Lanes 13-17 correspond to the effluent lysate, 137 mM NaCl wash, 500 mM NaCl wash, 100 mM acetate buffer wash and 5% formic acid elution, respectively, on an anti-HA membrane. The membrane diameters were 1.0 cm.

### 3.3.3 C-peptide capture in membranes containing immobilized anti-(C-peptide) antibody

Initially, I attempted to capture C-peptide in porous nylon membranes, but control experiments revealed non-specific adsorption of C-peptide to these membranes. ELISA quantification showed removal of over 50% of the C-peptide in 200 μL of 25 nM C-peptide passing through the bare nylon (Figure 3.8). Bare polyester (track-etched, pore size=0.4 μm) membranes showed similar C-peptide removal. PC membranes, however, exhibited no significant non-specific binding. Therefore, I selected PC membranes for subsequent

experiments. I should note that the track-etched PC membranes have a much lower porosity (4-20%) and thickness (10 μm) and, thus, lower surface area which will reduce both non-specific and specific binding.

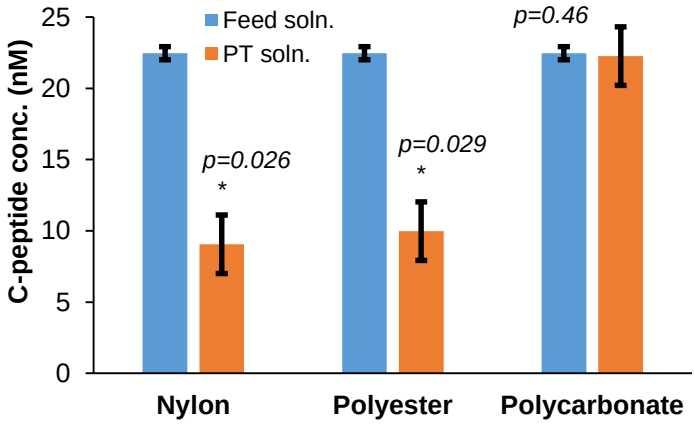


**Figure 3.8.** Concentrations of C-peptide before (feed, blue bars) and after (effluent, orange bars) passing through bare nylon, polyester and PC membranes. 200 μL of 25 nM C-peptide was passed through each membrane, and C-peptide in the feed and effluent solutions was quantified using ELISA.

The amount of anti-(C-peptide) immobilization should allow capture of as much as 280 pmoles of C-peptide. (This value assumes a 1:1 binding in a 0.4 μm membrane with a diameter of 1.0 cm.) After passage of 200 μL of 25 nM C-peptide through anti-(C-peptide) containing membranes, effluent concentrations were 17.0 ± 2.9 nM and 5.01 ± 0.8 nM for membranes with 1.0 μm and 0.4 μm pores, respectively (see Figure 3.9). Control experiments showed significant non-specific adsorption with 1.0 μm pores containing PAA/PEI/PAA films, whereas no significant non-specific adsorption occurred with membranes containing 0.4 μm pores modified with just PAA. The adsorption of C-peptide to PAA/PEI/PAA films but not to a single PAA layer stem from the positive PEI ammonium groups that electrostatically bind the negatively-charged C-peptide.

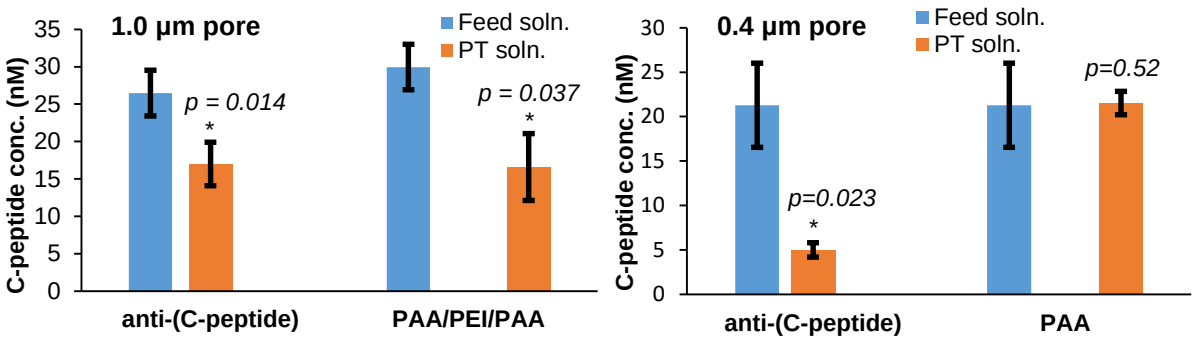


**Figure 3.9.** C-peptide concentrations before (feed, blue) and after (PT, orange) passing through 1.0 µm pore (left) and 0.4 µm pore (right) membranes. The 0.4 µm pore membranes bound more C-peptide than 1.0 µm pore membranes. Also, the PAA/PEI/PAA control membranes for the 1.0 µm pore membranes bound a significant amount of C-peptide, whereas the PAA control membranes for 0.4 µm pore membranes did not bind a significant amount of C-peptide.

### 3.4 Conclusions

A two-step procedure, electrostatic adsorption to polyelectrolytes followed by covalent binding successfully immobilizes both anti-HA and anti-(C-peptide) antibodies in membranes. Based on the decrease in absorbance of anti-HA solutions after circulating through the membrane, nylon membranes modified with PAA/PEI/PAA capture 75% of anti-HA in the feed solution. Anti-(C-peptide) capture was up to 53.1 mg/mL in 1.0 µm pore PC membranes modified with PAA/PEI/PAA films and 0.4 µm pore PC membranes modified with PAA. The similar capacities suggest that 0.4 µm pore membranes are the better candidate for C-peptide capture due to shorter radial diffusion to binding sites within the pores.

The anti-HA containing membranes successfully capture HA-RGS2 protein, but non-specific binding also occurs. Due to the low HA-RGS2 concentration, non-specifically bound protein may interfere with downstream analyses, masking signals from HA-RGS2. Although increasingly stringent buffer washes remove non-specifically bound proteins, SDS-PAGE still

shows many unwanted proteins in the eluate. Importantly, 5% formic acid is an effective eluent that is compatible with subsequent mass spectrometry.

The presence of significant non-specific adsorption with HA lysate and anti-HA membranes and the absence thereof with NT lysate is perplexing. Gel electrophoresis suggests that initial HA-RGS2 binding to the anti-HA membrane causes subsequent non-specific adsorption. However, we do not think that specific protein binding to bound RGS2 causes this phenomenon, because RGS2 is present in very small amounts that are undetectable via gel electrophoresis. A more likely explanation is that bound RGS2 creates a hydrophobic layer on the membrane surface, allowing other proteins to associate via hydrophobic interactions. Perhaps as layer upon layer of protein associates with the surface via hydrophobic interactions, eventually an assortment of proteins in large excess to RGS2 builds up on the membrane and elutes in 5% formic acid.

Initial studies with bare nylon membranes for C-peptide capture revealed significant non-specific adsorption of C-peptide. Subsequent experiments with bare polyester and polycarbonate membranes revealed that only PC exhibits no significant non-specific binding. Nevertheless, 1.0 μm pore membranes modified with PAA/PEI/PAA films exhibited significant non-specific adsorption, whereas the 0.4 μm pore PC membranes modified with only a single PAA layer showed no significant non-specific adsorption. The non-specific adsorption to PAA/PEI/PAA films may stem from the positively-charged PEI layer electrostatically binding negatively-charged C-peptide. The 0.4 μm pore membranes containing PAA-anti-(C-peptide) also bound significantly more C-peptide than 1.0 μm pore membranes modified with PAA/PEI/PAA-anti-(C-peptide). Perhaps the small pores bind more C-peptide due to short radial diffusion distances to pore walls. Rapid capture of C-peptide during pumping of low concentrations of C-peptide

through the membrane bodes well for future capture of C-peptide in microfluidic devices where the C-peptide slowly diffuses through the membrane. Nevertheless, we do not know if the anti-(C-peptide) antibody exhibits any non-specific adsorption of other proteins. Therefore, future experiments will test for non-specific adsorption of insulin and $Zn^{2+}$ - the two pancreatic cell secretion ingredients that seem to affect red blood cell ATP release and glucose clearance.[25,26]

# REFERENCES

REFERENCES


(1) Cuatrecasas, P. Protein Purification by Affinity Chromatography. *J. Biochem. Biophys. Methods* **1970**, *245* (12), 3059–3065.

(2) Zou, H.; Luo, Q.; Zhou, D. Affinity Membrane Chromatography for the Analysis and Purification of Proteins. *J. Biochem. Biophys. Methods* **2001**, *49* (1-3), 199–240.

(3) Bruening, M. L.; Dotzauer, D. M.; Jain, P.; Ouyang, L.; Baker, G. L. Creation of Functional Membranes Using Polyelectrolyte Multilayers and Polymer Brushes. *Langmuir* **2008**, *24* (15), 7663–7673.

(4) Huang, W.; Kim, J. B.; Bruening, M. L.; Baker, G. L. Functionalization of Surfaces by Water-Accelerated Atom-Transfer Radical Polymerization of Hydroxyethyl Methacrylate and Subsequent Derivatization. *Macromolecules* **2002**, *35* (4), 1175–1179.

(5) Dai, J.; Bao, Z.; Sun, L.; Hong, S. U.; Baker, G. L.; Bruening, M. L. High-Capacity Binding of Proteins by Poly(acrylic Acid) Brushes and Their Derivatives. *Langmuir* **2006**, *22* (9), 4274–4281.

(6) Dai, J.; Baker, G. L.; Bruening, M. L. Use of Porous Membranes Modified with Polyelectrolyte Multilayers as Substrates for Protein Arrays with Low Nonspecific Adsorption. *Anal. Chem.* **2006**, *78* (1), 135–140.

(7) Waugh, D. S. Making the Most of Affinity Tags. *Trends Biotechnol.* **2005**, *23* (6), 316–320.

(8) Young, C. L.; Britton, Z. T.; Robinson, A. S. Recombinant Protein Expression and Purification: A Comprehensive Review of Affinity Tags and Microbial Applications. *Biotechnol. J.* **2012**, *7* (5), 620–634.

(9) Lichty, J. J.; Malecki, J. L.; Agnew, H. D.; Michelson-Horowitz, D. J.; Tan, S. Comparison of Affinity Tags for Protein Purification. *Protein Expr. Purif.* **2005**, *41* (1), 98–105.

(10) Arnau, J.; Lauritzen, C.; Petersen, G. E.; Pedersen, J. Current Strategies for the Use of Affinity Tags and Tag Removal for the Purification of Recombinant Proteins. *Protein Expr. Purif.* **2006**, *48* (1), 1–13.

(11) Ning, W.; Wijeratne, S.; Dong, J.; Bruening, M. L. Immobilization of Carboxymethylated Polyethylenimine-Metal-Ion Complexes in Porous Membranes to Selectively Capture His-Tagged Protein. *ACS Appl. Mater. Interfaces* **2015**, *7* (4), 2575–2584.

(12) Bhattacharjee, S.; Dong, J.; Ma, Y.; Hovde, S.; Geiger, J. H.; Baker, G. L.; Bruening, M. L. Formation of High-Capacity Protein-Adsorbing Membranes through Simple

Adsorption of Poly(acrylic Acid)-Containing Films at Low pH. *Langmuir* **2012**, *28* (17), 6885–6892.

(13) Bhut, B. V.; Conrad, K. A.; Husson, S. M. Preparation of High-Performance Membrane Adsorbers by Surface-Initiated AGET ATRP in the Presence of Dissolved Oxygen and Low Catalyst Concentration. *J. Memb. Sci.* **2012**, *390-391*, 43–47.

(14) Boi, C. Membrane Adsorbers as Purification Tools for Monoclonal Antibody Purification. *J. Chromatogr. B. Analyt. Technol. Biomed. Life Sci.* **2007**, *848* (1), 19–27.

(15) Ghosh, R. Protein Separation Using Membrane Chromatography: Opportunities and Challenges. *J. Chromatogr. A* **2002**, *952* (1-2), 13–27.

(16) Ning, W.; Bruening, M. L. Rapid Protein Digestion and Purification with Membranes Attached to Pipet Tips. *Anal. Chem.* **2015**, *87* (24), 11984–11989.

(17) Dong, J. Functionalized Porous Membranes for Rapid Protein Purification and Controlled Protein Digestion Prior to Mass Spectrometry Analysis, Ph.D. Dissertation, Michigan State University, 2014.

(18) Jain, P.; Vyas, M. K.; Geiger, J. H.; Baker, G. L.; Bruening, M. L. Protein Purification with Polymeric Affinity Membranes Containing Functionalized Poly(acid) Brushes. *Biomacromolecules* **2010**, *11* (4), 1019–1026.

(19) Qu, Z.; Chen, K.; Gu, H.; Xu, H. Covalent Immobilization of Proteins on 3D Poly(acrylic Acid) Brushes: Mechanism Study and a More Effective and Controllable Process. *Bioconjug. Chem.* **2014**, *25* (2), 370–378.

(20) Nunn, C.; Zou, M.-X.; Sobiesiak, A. J.; Roy, A. A.; Kirshenbaum, L. A.; Chidiac, P. RGS2 Inhibits Beta-Adrenergic Receptor-Induced Cardiomyocyte Hypertrophy. *Cell. Signal.* **2010**, *22* (8), 1231–1239.

(21) Tuomi, J. M.; Chidiac, P.; Jones, D. L. Evidence for Enhanced M3 Muscarinic Receptor Function and Sensitivity to Atrial Arrhythmia in the RGS2-Deficient Mouse. *Am. J. Physiol. Heart Circ. Physiol.* **2010**, *298* (2), H554–H561.

(22) Raveh, A.; Schultz, P. J.; Aschermann, L.; Carpenter, C.; Tamayo-Castillo, G.; Cao, S.; Clardy, J.; Neubig, R. R.; Sherman, D. H.; Sjogren, B. Identification of Protein Kinase C Activation as a Novel Mechanism for RGS2 Protein Upregulation through Phenotypic Screening of Natural Product Extracts. *Mol. Pharmacol.* **2014**, *86* (4), 406–416.

(23) Lyu, J. H.; Park, D. W.; Huang, B.; Kang, S. H.; Lee, S. J.; Lee, C.; Bae, Y. S.; Lee, J. G.; Baek, S. H. RGS2 Suppresses Breast Cancer Cell Growth via a MCPIP1-Dependent Pathway. *J. Cell. Biochem.* **2015**, *116* (2), 260–267.

(24) Steiner, D. F.; Cunningham, D.; Spigelman, L.; Aten, B. Insulin Biosynthesis: Evidence for a Precursor. *Science* **1967**, *157* (3789), 697–700.

(25) Meyer, J. A.; Froelich, J. M.; Reid, G. E.; Karunarathne, W. K. A.; Spence, D. M. Metal-Activated C-Peptide Facilitates Glucose Clearance and the Release of a Nitric Oxide Stimulus via the GLUT1 Transporter. *Diabetologia* **2008**, *51* (1), 175–182.

(26) Liu, Y.; Chen, C.; Summers, S.; Medawala, W.; Spence, D. M. C-Peptide and Zinc Delivery to Erythrocytes Requires the Presence of Albumin: Implications in Diabetes Explored with a 3D-Printed Fluidic Device. *Integr. Biol.* **2015**, *7* (5), 534–543.

# Chapter 4. Research summary and future work

## 4.1 Research summary

This thesis describes the development of membrane-based platforms for antibody purification and detection and immunoprecipitation. After adsorption of polyelectrolyte films in membrane pores, I linked small peptides and antibodies to these immobilized polyelectrolytes to create materials that capture specific proteins. Chapter 2 describes covalent immobilization of small, antibody-binding peptides for antibody purification and detection. I added spacer arms to the peptides along with lysine residues for covalent linking to the carboxylic acid groups of adsorbed PAA. The peptide immobilization amounts were 57.6 ± 0.3 mg/mL for KK12 and 27.4 ± 4.0 mg/mL for K19. The greater immobilization of KK12 compared to K19 may stem from two, rather than one, lysine residues in the peptide or the shorter peptide length (12 vs. 19 amino acids). The Fc-binding peptide KK12 captured 8.40 mg of Herceptin and 9.96 mg of Avastin per mL membrane. The antibodies eluted in 100 mM Gly, but the membranes were not reusable. Reused membranes exhibited an average binding capacity of at most 2.3 mg/mL. For such membranes to present a viable alternative to protein A and protein G columns, future research must examine membrane reuse and increase capacity.

The Fab-binding peptide K19 specifically bind 16.3 ± 1.14 mg of Herceptin per mL membrane, whereas the Avastin binding capacity is only 2.6 mg/mL, and this value may in part reflect dead volume in the system and not actual binding. K19-modified membranes selectively purify Herceptin from human serum, suggesting that membrane-bound Fab-binding peptides

may enable rapid, specific antibody detection in human serum to monitor therapeutic antibody clearance in patients.

Chapter 3 describes the development of antibody-containing membranes for immunoprecipitation. Both tagged proteins and native antigens bind to membrane-immobilized antibodies. Antibody immobilization occurred via electrostatic immobilization followed by covalent linking, and we monitored antibody immobilization via NanoDrop UV/Vis spectroscopy. Immobilized anti-HA antibodies in nylon membranes capture HA-tagged RGS2 protein. However, non-specific binding is a persistent problem that we need to address for downstream analyses. PC membranes containing anti-(C-peptide) antibodies captured C-peptide and exhibited low non-specific binding, and these membranes should facilitate studies of how C-peptide secretions affect red blood cells.

## 4.2 Future work

### 4.2.1 Acid-labile linker for universal low pH elution

The antibodies employed in this research are well-known therapeutic drugs. As such, they exhibit very high-affinities for their corresponding antigens. Thus, as one might expect, Herceptin also shows a high affinity for the HER2-mimetic peptide K19. The interaction is so strong, however, that we could only elute Herceptin with detergent containing a reductant (2% SDS, 100 mM DTT). Such highly-denaturing elution conditions will make downstream quantitative analyses very difficult, and cumbersome SDS-removal methods such as dialysis often result in significant sample loss.[1] The small elution volumes and sample mass necessitate a different approach. Although other methods of detergent removal exist,[2,3] few are amenable to

such small volumes and high SDS content. Furthermore, each of these SDS removal methods add additional costs to antibody purification and analysis. Therefore, future work should focus on alternative elution methods. The ideal elution method should be inexpensive, effective and universal with no downstream interferences. Thus, we are aiming to develop an acid-labile linker to enable universal elution of affinity molecules (and their associated proteins) at low pH. We prepared an acid-labile linker using *cis*-aconitic anhydride (cisA) according to a literature method[4] (see Figure 4.1) and employed low-pH elution of Herceptin from K19-modified membranes.

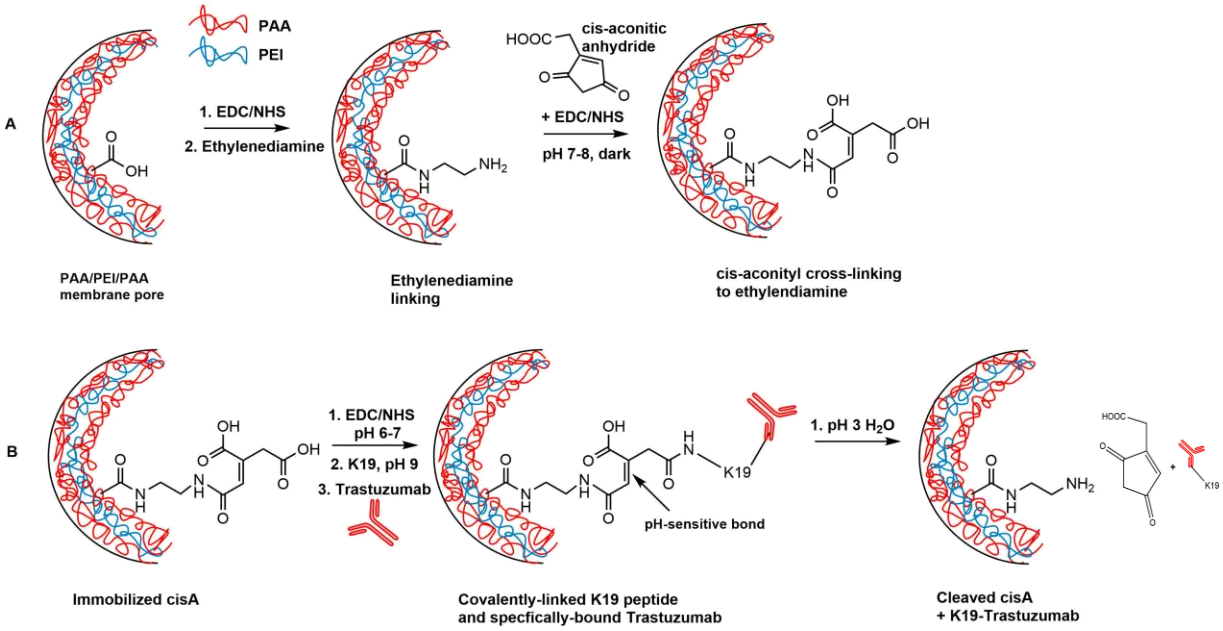


**Figure 4.1.** Reaction scheme for (A) cis-aconitic anhydride linking to the membrane and (B) subsequent activation, covalent peptide immobilization, antibody capture and acidic elution. The pH-sensitive bond in cisA cleaves at approximately pH 5.

### 4.2.1.1 Acid-labile linker experimental methods

*Films on Au-coated wafers.* After deposition of MPA monolayers and $(PEI/PAA)_2$ films on Au-coated Si wafers, the wafers were immersed in 5 mL of 0.1 M EDC/NHS for 1 hour and

subsequently rinsed with deionized water, dried with $N_2$ and examined via reflectance FTIR spectroscopy to confirm successful activation. The activated wafers were subsequently exposed to 5 mL of 100 mM ethylenediamine (pH 10) for 2 hours, rinsed with deionized water, dried with $N_2$ and again examined via reflectance FTIR spectroscopy. The ethylenediamine-modified wafers were placed in pH 3 water for 30 minutes for acidification, rinsed with pH 3 water and dried with $N_2$ prior to FTIR spectroscopy. In a separate vial wrapped in aluminum foil to block all light, a solution of 100 mM cis-aconitic anhydride (cisA) in 5 mL of 0.1 M EDC/NHS (pH 7) was allowed to react for 1 hour. After 1 hour of cisA activation, the ethylenediamine-modified wafers were immersed in the solution and allowed to sit overnight. The wafers were subsequently rinsed with deionized water, dried with $N_2$ and examined via reflectance FTIR spectroscopy to confirm cisA immobilization. To test the cleavage of the pH-sensitive cisA linker, the cisA-modified wafers were immersed in 5 mL of pH 3 water (adjusted by dropwise addition of 0.1 M HCl) for 30 minutes and subsequently rinsed with pH 3 water and then deionized water, dried with $N_2$ and examined via reflectance FTIR spectroscopy.

*Membranes*. After deposition of PAA/PEI/PAA films in nylon membranes, 5 mL of 0.1 M EDC/NHS solution was circulated through the membrane for 1 hour at a flow rate of 1.0 mL/min to convert PAA carboxylic acid groups to NHS esters and subsequently rinsed with 5 mL of deionized. A 5 mL, 100 mM ethylenediamine solution was then circulated through the membrane for 2 h. The membrane was subsequently washed with deionized water for 10 minutes. In a separate vial wrapped in aluminum foil to block light, a solution of 100 mM cis-aconitic anhydride (cisA) in 5 mL of 0.1 M EDC/NHS (pH 7) was allowed to react for 1 hour. After wrapping the circulation tubing in foil, the solution of activated cisA was circulated through the membrane for 3 hours. The membrane was subsequently washed with deionized

water for 10 minutes. A 5 mL, 0.1 M EDC/NHS solution was prepared and adjusted to pH 7 by the dropwise addition of 0.1 M NaOH. This 0.1 M EDC/NHS solution was then circulated through the membrane for 1 hour to activate the cisA-modified membrane. A 1 mg/mL K19 feed solution was obtained by dissolving 2 mg peptide in 2 mL water, and the pH of this solution was adjusted to 8-9 by dropwise addition of 0.1 M NaOH. The peptide solution was circulated through the activated membrane for 2 h, and the membrane was subsequently washed with deionized water for 10 minutes. The feed and effluent (circulated) solutions were both diluted 1:9 and analyzed via fluorescence spectroscopy as outlined in section 2.2.3 to determine K19 capture on the cisA-membrane. The cisA-K19-modified membrane was subsequently washed with 5 mL of 20 mM PBS (137 mM NaCl, pH 7.4), and a 0.1 mg/mL solution of Herceptin in 20 mM PBS (137 mM NaCl, pH 7.4) was passed through the membrane at a flow rate of 0.5 mL/min. After washing with 1 mL aliquots of 20 mM PBS (137 mM NaCl, pH 7.4) and 20 mM PBS (500 mM NaCl, pH 7.4), Herceptin was eluted from the membrane in 150 μL of pH 3 water (prepared via dropwise addition of 0.1 M HCl to deionized water). The Herceptin binding on the cisA-K19-modified membrane was determined via breakthrough curves using a Bradford assay as outlined in section 2.2.4.

#### 4.2.1.2 Acid-labile linker results and discussion

I first anchored the acid-labile linker to PEMs on Au-coated Si wafers to enable monitoring of each step of the reaction sequence via reflectance FTIR spectroscopy. After activation of $(PEI/PAA)_2$ polyelectrolyte films with EDC/NHS, reaction with ethylenediamine should yield free amine groups near the film surface. I added ethylenediamine in excess to both minimize cross-linking and effectively react with all PAA carboxylic acid groups. Figure 4.2. shows the

FTIR spectrum of the film after reaction with ethylenediamine and acidification. The strong amide I and II bands at 1660 $cm^{-1}$ and 1560 $cm^{-1}$, respectively, confirm the reaction of ethylenediamine with -COOH groups to form amides. After activation of cisA with EDC/NHS in the dark and under neutral conditions for 1 hour, amine groups should react with the activated cisA to immobilize the linker. The increase in the peak at 1710 $cm^{-1}$ after reaction with activated cisA suggests the presence of new carboxylic acid groups on the wafer. Under the neutral conditions of reaction with cisA the rise in this peak should not correspond to newly-protonated PAA carboxylic acid groups, especially when compared to the acidified ethylenediamine spectrum. However, the amide bands do not increase as much as expected. After cisA modification, I placed the wafers in pH 3 water to cleave the cisA linker from the ethylenediamine. The reduction in the carboxylic acid peak at 1710 $cm^{-1}$ under acidic conditions suggests that the cisA cleaved from the wafer and, as expected, the FTIR spectrum appeared almost identical to the acidified spectrum after reaction with ethylendiamine. Furthermore, the subtle increase in amide I (1660 $cm^{-1}$) and amide II (1560 $cm^{-1}$) peaks after cisA exposure and

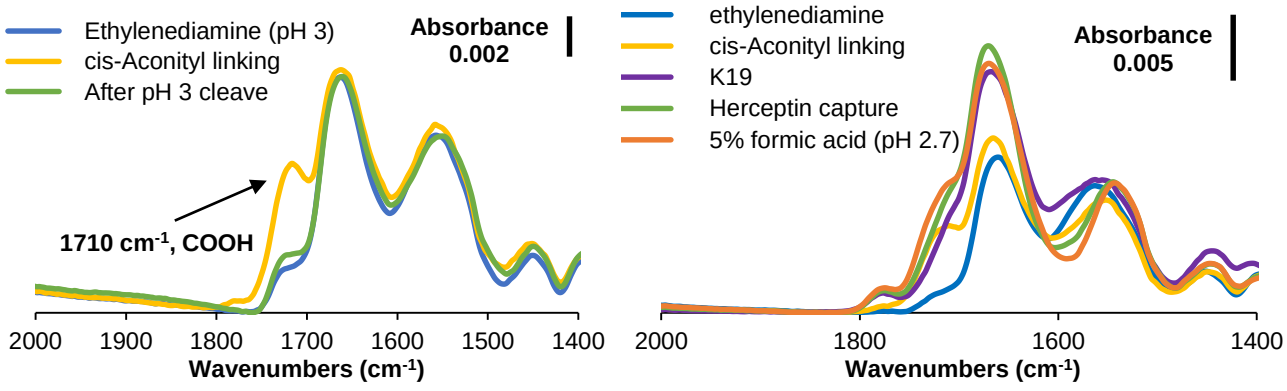


**Figure 4.2.** (A) FTIR spectra of $(PEI/PAA)_2$ films on MPA-modified, Au-coated Si wafers during the sequence for *cis*-aconityl modification and its cleavage from the wafer. The significant increase in the peak at 1720 $cm^{-1}$ under basic conditions and its return to the ethylenediamine level under acidic conditions suggests successful *cis*-aconityl modification and cleavage. (B) FTIR spectra of $(PEI/PAA)_2$-cisA films after covalent linking of K19 to *cis*-aconityl, subsequent Herceptin capture and immersion in 5% formic acid (pH 2.7).

subtle decrease after subsequent pH 3 water exposure are consistent with the formation and cleavage of amide bonds.

I performed K19 immobilization on cisA-modified wafers that were not immersed in the pH 3.0 solution. A large increase in the amide absorbance after activation of the cisA -COOH groups and reaction with K19 (Figure 4.2b) confirms immobilization of the peptide. Moreover, a subsequent increase in the amide bond after immersion in a Herceptin solution is consistent with capture of a small amount of antibody. However, we did not see cleavage of the cisA linker after immersing the wafer in 5% formic acid (pH 2.7) for 30 minutes. There was a subtle decrease in the amide bond peak after immersion in 5% formic acid, perhaps due to changes in the pH rather than loss of antibody. The lack of elution of peptide and protein at pH 2.7 may suggest that the K19 is not covalently immobilized to the cisA linker.

Immobilization of cisA in membranes is difficult to monitor. Because ethylenediamine should react with nearly all free PAA carboxyl groups, however, the K19 immobilization results should provide some idea of how much cisA was linked to the membrane. Unfortunately, membranes with activated (PAA/PEI/PAA)-cisA films captured only 3.4 mg of K19 per mL of membrane. Thus, the cisA linking procedure is not yet robust. The larger membrane (2.5 cm diameter, 0.0346 $cm^3$ vol.) was cut for a smaller membrane (1.0 cm diameter, 0.00864 $cm^3$ vol.) to be used for a Bradford assay breakthrough curve (see Figure 4.3). The cisA-K19 membrane captured just 1.27 mg Herceptin per mL membrane, a very low binding capacity when compared with the non-cisA, K19-modified membranes which capture 16.1 mg Herceptin per mL membrane.

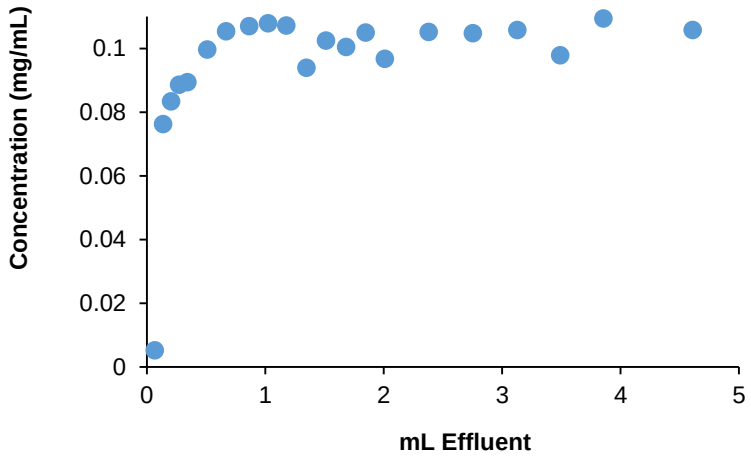


**Figure 4.3.** Bradford assay breakthrough curve for passage of 0.1 mg/mL Herceptin through a 1.0 cm diameter membrane modified with PAA/PEI/PAA-cisA-K19. The binding capacity was calculated to be 1.27 mg/mL.

### 4.2.2 HA-RGS2 purification using a membrane with an immobilized Fc-binding peptide

Section 3.3.2 described capture of HA-tagged RGS2 in membranes containing immobilized anti-HA antibodies. However, non-specific binding presented problems for downstream analyses even after increasingly aggressive buffer washes. The anti-HA antibody we employed in the HA-RGS2 purification was polyclonal. Although polyclonal antibodies are typically better for immunoprecipitation because they can bind to different parts of the target antigen and, thus, offer a greater capacity, they may also exhibit affinity for other proteins in the cell lysate.[5] Employing a monoclonal, anti-HA antibody might reduce non-specific binding and, therefore, result in higher purity proteins for downstream analysis. Also, employing an indirect immunoprecipitation[5-7] method wherein anti-HA antibody is first exposed to cell lysate in solution and the anti-HA-HA-RGS2 complex is subsequently captured via a membrane-bound Fc-binding peptide (see section 2.3.2) may offer reduced non-specific binding and a greater capacity. Future research in this area may use the KK12 Fc-binding peptide to capture anti-HA-HA-RGS2. However, several Fc-binding peptides have been identified and need to be

evaluated.[8-13] Future work in this area may determine the most effective Fc-binding peptides for antibody capture and indirect immunoprecipitation.

### 4.2.3 C-peptide capture from cell secretions on membranes implanted in a 3D-printed microfluidic cell

Section 3.3.3 described my initial efforts for C-peptide capture with anti-(C-peptide) membranes. Those results show successful C-peptide capture with 0.4 μm PC membranes and minimal C-peptide binding to control membranes. However, ultimately this research aims to selectively capture C-peptide from cell secretions. We do not yet know whether the anti-(C-peptide) membranes will non-specifically adsorb other cell secretion components, specifically insulin and $Zn^{2+}$. The results from the anti-HA membrane experiments (see section 3.3.2) suggest that non-specific adsorption could be a problem. To test for non-specific adsorption of insulin and $Zn^{2+}$, we can pass cocktails of equimolar C-peptide, insulin and $Zn^{2+}$ through an anti-(C-peptide) membrane and subsequently determine C-peptide and insulin concentrations via ELISA, and $Zn^{2+}$ concentration using TSQ fluorescence spectroscopy.

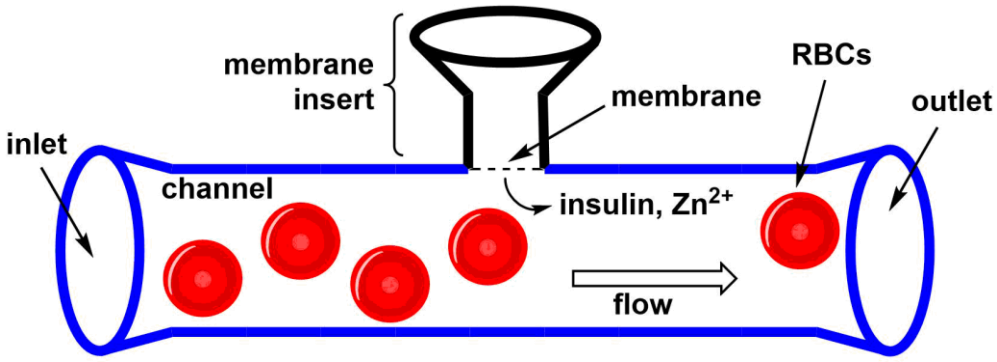


**Figure 4.4.** Schematic drawing of a microfluidic device with a membrane insert. As cell secretions diffuse across the membrane and into the channel, an anti-(C-peptide) membrane can capture the C-peptide.

Ultimately, we will place anti-(C-peptide) membranes in microfluidic devices wherein the membrane lies parallel with the direction of flow (see Figure 4.4). Cell culture excretions from the top of the membrane can diffuse through the membrane pores and into the channels. Capturing C-peptide from these secretions may provide insight into C-peptide's role in red blood cell ATP release, glucose clearance and cell-to-cell communications.[14]

### 4.3 Impact

The membrane-based separations techniques described in this thesis provide innovative platforms for antibody purification and immunoprecipitation. The KK12 modified membranes are the first step toward a rapid, affordable alternative to protein A and protein G chromatographic columns. More research needs to be done with Fc-binding peptides, though, to develop a viable alternative. Several Fc-binding peptide candidates exist,[8-13,15-17] and one can assess their binding capacities, elutions and reusabilities to determine which Fc-binding peptide is the most promising alternative to protein A and protein G columns. The K19 membranes selectively bind Herceptin in blood serum and, thus, can be used for detection after treatment. Quantifying Herceptin levels in blood serum may save patients thousands of dollars in unnecessary treatments, and rapid techniques are crucial for such time-sensitive measurements. However, implementation of membranes for Herceptin quantification will require a more effective elution protocol. There are other opportunities for mimotope-modified membranes for detection in blood serum, such as the CD20 mimotope for Rituximab (Rituxan).[18] Applying this research to other systems could lead to the development of a portfolio of rapid therapeutic antibody detection membranes.

Membrane-based immunoprecipitation techniques offer a rapid alternative to traditional immunoprecipitation columns. Antibody immobilization was successful for both anti-HA and anti-(C-peptide) antibodies in both nylon and PC membranes, and the membranes captured HA-RGS2 and C-peptide in a fraction of the time required for traditional immunoprecipitation columns. Non-specific binding was a persistent problem, however, with complicated mixtures such as cell lysate. Further research may optimize antibody membranes for lower non-specific binding and greater capacity and establish immunoprecipitation membranes as convenient, rapid alternatives to immunoprecipitation columns.

This research focused primarily on developing membrane-based platforms that manipulated antibody-antigen interactions for purification and detection. As more therapeutic antibodies become available, purification and detection will become even more important. Protein isolation with the membrane-based platforms discussed in this thesis is faster than traditional techniques and, perhaps, uniquely suited for the future of antibody research.

# REFERENCES

REFERENCES


(1) Sousa, M. M.; Steen, K. W.; Hagen, L.; Slupphaug, G. Antibody Cross-Linking and Target Elution Protocols Used for Immunoprecipitation Significantly Modulate Signal-to Noise Ratio in Downstream 2D-PAGE Analysis. *Proteome Sci.* **2011**, *9* (1), 45.

(2) Fox, J. L.; Stevens, S. E.; Taylor, C. P.; Poulsen, L. L. SDS Removal from Protein by Polystyrene Beads. *Anal. Biochem.* **1978**, *87* (1), 253–256.

(3) Rigaud, J. L.; Levy, D.; Mosser, G.; Lambert, O. Detergent Removal by Non-Polar Polystyrene Beads: Applications to Membrane Protein Reconstitution and Two-Dimensional Crystallization. *Eur. Biophys. J.* **1998**, *27* (4), 305–319.

(4) Battogtokh, G.; Ko, Y. T. Active-Targeted pH-Responsive Albumin–photosensitizer Conjugate Nanoparticles as Theranostic Agents. *J. Mater. Chem. B* **2015**, *3* (48), 9349–9359.

(5) Bonifacino, J. S.; Dell'Angelica, E. C.; Springer, T. A. Immunoprecipitation. In *Current Protocols in Immunology*; John Wiley & Sons, Inc., 2001; pp 8.3.1–8.3.28.

(6) Otto, J. J.; Lee, S. W. Immunoprecipitation Methods. *Methods Cell Biol.* **1993**, *37*, 119–127.

(7) Kessler, S. W. *Immunochemical Techniques: Part B*; Methods in Enzymology; Elsevier, 1981; Vol. 73, pp. 442-459.

(8) Yang, H.; Gurgel, P. V.; Carbonell, R. G. Purification of Human Immunoglobulin G via Fc-Specific Small Peptide Ligand Affinity Chromatography. *J. Chromatogr. A* **2009**, *1216* (6), 910–918.

(9) Jeong, Y. jin; Kang, H. J.; Bae, K. H.; Kim, M. G.; Chung, S. J. Efficient Selection of IgG Fc Domain-Binding Peptides Fused to Fluorescent Protein Using E. Coli Expression System and Dot-Blotting Assay. *Peptides* **2010**, *31* (2), 202–206.

(10) Sugita, T.; Katayama, M.; Okochi, M.; Kato, R.; Ichihara, T.; Honda, H. Screening of Peptide Ligands That Bind to the Fc Region of IgG Using Peptide Array and Its Application to Affinity Purification of Antibody. *Biochem. Eng. J.* **2013**, *79*, 33–40.

(11) Tsai, C. W.; Jheng, S. L.; Chen, W. Y.; Ruaan, R. C. Strategy of Fc-Recognizable Peptide Ligand Design for Oriented Immobilization of Antibody. *Anal. Chem.* **2014**, *86* (6), 2931–2938.

(12) Lund, L. N.; Gustavsson, P. E.; Michael, R.; Lindgren, J.; Nørskov-Lauritsen, L.; Lund, M.; Houen, G.; Staby, A.; St. Hilaire, P. M. Novel Peptide Ligand with High Binding Capacity for Antibody Purification. *J. Chromatogr. A* **2012**, *1225*, 158–167.

(13) Wei, Y.; Xu, J.; Zhang, L.; Fu, Y.; Xu, X. Development of Novel Small Peptide Ligands for Antibody Purification. *RSC Adv.* **2015**, *5* (82), 67093–67101.

(14) Meyer, J. A.; Froelich, J. M.; Reid, G. E.; Karunarathne, W. K. A.; Spence, D. M. Metal-Activated C-Peptide Facilitates Glucose Clearance and the Release of a Nitric Oxide Stimulus via the GLUT1 Transporter. *Diabetologia* **2008**, *51* (1), 175–182.

(15) Kim, K. J.; Li, B.; Houck, K.; Winer, J.; Ferrara, N. The Vascular Endothelial Growth Factor Proteins: Identification of Biologically Relevant Regions by Neutralizing Monoclonal Antibodies. *Growth Factors* **1992**, *7* (1), 53–64.

(16) Presta, L. G.; Chen, H.; O'Connor, S. J.; Chisholm, V.; Meng, Y. G.; Krummen, L.; Winkler, M.; Ferrara, N. Humanization of an Anti-Vascular Endothelial Growth Factor Monoclonal Antibody for the Therapy of Solid Tumors and Other Disorders. *Cancer Res.* **1997**, *57* (20), 4593–4599.

(17) Zhao, W. W.; Shi, Q. H.; Sun, Y. FYWHCLDE-Based Affinity Chromatography of IgG: Effect of Ligand Density and Purifications of Human IgG and Monoclonal Antibody. *J. Chromatogr. A* **2014**, *1355*, 107–114.

(18) Leo, N.; Shang, Y.; Yu, J.; Zeng, X. Characterization of Self-Assembled Monolayers of Peptide Mimotopes of CD20 Antigen and Their Binding with Rituximab. *Langmuir* **2015**, *31* (51), 13764–13772.